



ANL-ART-261  
ANL-METL-43

## **Thermal Hydraulic Experimental Test Article – Fiscal Year 2022 Final Report**

---

**Nuclear Sciences and Engineering Division**

### **About Argonne National Laboratory**

Argonne is a U.S. Department of Energy laboratory managed by UChicago Argonne, LLC under contract DE-AC02-06CH11357. The Laboratory's main facility is outside Chicago, at 9700 South Cass Avenue, Argonne, Illinois 60439. For information about Argonne and its pioneering science and technology programs, see [www.anl.gov](http://www.anl.gov).

### **DOCUMENT AVAILABILITY**

**Online Access:** U.S. Department of Energy (DOE) reports produced after 1991 and a growing number of pre-1991 documents are available free at OSTI.GOV (<http://www.osti.gov/>), a service of the US Dept. of Energy's Office of Scientific and Technical Information.

### **Reports not in digital format may be purchased by the public from the National Technical Information Service (NTIS):**

U.S. Department of Commerce  
National Technical Information  
Service 5301 Shawnee Rd  
Alexandria, VA 22312  
**[www.ntis.gov](http://www.ntis.gov)**  
Phone: (800) 553-NTIS (6847) or (703) 605-6000  
Fax: (703) 605-6900  
Email: **[orders@ntis.gov](mailto:orders@ntis.gov)**

### **Reports not in digital format are available to DOE and DOE contractors from the Office of Scientific and Technical Information (OSTI):**

U.S. Department of Energy  
Office of Scientific and Technical Information  
P.O. Box 62  
Oak Ridge, TN 37831-0062  
**[www.osti.gov](http://www.osti.gov)**  
Phone: (865) 576-8401  
Fax: (865) 576-5728  
Email: **[reports@osti.gov](mailto:reports@osti.gov)**

### **Disclaimer**

This report was prepared as an account of work sponsored by an agency of the United States Government. Neither the United States Government nor any agency thereof, nor UChicago Argonne, LLC, nor any of their employees or officers, makes any warranty, express or implied, or assumes any legal liability or responsibility for the accuracy, completeness, or usefulness of any information, apparatus, product, or process disclosed, or represents that its use would not infringe privately owned rights. Reference herein to any specific commercial product, process, or service by trade name, trademark, manufacturer, or otherwise, does not necessarily constitute or imply its endorsement, recommendation, or favoring by the United States Government or any agency thereof. The views and opinions of document authors expressed herein do not necessarily state or reflect those of the United States Government or any agency thereof, Argonne National Laboratory, or UChicago Argonne, LLC.

# **Thermal Hydraulic Experimental Test Article – Fiscal Year 2022 Final Report**

---

**M. Weathered, C. Grandy, D. Kultgen, E. Kent, J. Rein, L. Ibarra**

Nuclear Sciences and Engineering Division  
Argonne National Laboratory

September 2022

## TABLE OF CONTENTS

|  |    |
|--|----|
| 1. Executive Summary .....                             | 1  |
| 2. Introduction .....                                  | 4  |
| 2.1. System Overview and Systems Code Application..... | 4  |
| 3. Primary System Development.....                     | 6  |
| 3.1. Primary Pump and Flowmeter .....                  | 7  |
| 3.2. Electrically Heated Core .....                    | 10 |
| 3.3. Data Acquisition and Control .....                | 16 |
| 4. Secondary System .....                              | 21 |
| 4.1. Piping Design.....                                | 21 |
| 4.2. Secondary Flowmeter .....                         | 22 |
| 4.3. Secondary Pump .....                              | 24 |
| 4.4. Intermediate Heat Exchanger.....                  | 25 |
| 4.5. Sodium to Air Heat Exchanger .....                | 26 |
| 5. Experimental Data Generation .....                  | 31 |
| 6. THETA Model Development.....                        | 36 |
| 7. Conclusions and Path Forward.....                   | 36 |
| 8. Acknowledgements .....                              | 37 |
| 9. References .....                                    | 38 |

## LIST OF FIGURES

|   |    |
|---|----|
| Figure 1: THETA primary system .....  | 2  |
| Figure 2: Isometric drawing of THETA secondary system .....   | 2  |
| Figure 3: THETA installed in METL test vessel #4. Left: uninsulated without pump motor installed. Right: insulated with pump motor installed. ....  | 3  |
| Figure 4: P&ID schematic of THETA .....   | 4  |
| Figure 5: THETA pool and core geometry. Core nominal diameter: 0.2 [m] (8”), core heated length: 0.3 [m] (12”) .....  | 5  |
| Figure 6: Schematic of SAS4A/SASSYS-1 showing locations of various compressible volumes (CV#) and segments (S#) .....   | 6  |
| Figure 7: Photo of THETA primary system cold pool components .....  | 7  |
| Figure 8: THETA pump speed vs time during sodium commissioning test # 2022-05-23-01 ...   | 8  |
| Figure 9: THETA flowmeter flowrate vs time during sodium commissioning test # 2022-05-23-01. Sodium temperature at pump inlet: 203.1 °C. Flowmeter magnet temperature: 193.1 °C. ....   | 8  |
| Figure 10: THETA flowrate vs pump speed during sodium commissioning test # 2022-05-23-01.....   | 9  |
| Figure 11: Photo of completed THETA submersible electromagnetic flowmeter with 15” ruler for reference. Note the 1/8” MI cables transmitting temperature and sensor data have been spooled up for easy transport.....   | 9  |
| Figure 12: Manufacturer supplied SSR panel.....   | 10 |
| Figure 13: Updated control panel for electrically heated core using phase angle fired SCR control. Top left shows the outside of the enclosure where the Schneider electric PM5110 power meter and dedicated over temperature controller are located. Top right shows the inside of the enclosure. Bottom shows the internals of the three phase SCR (PN: Ametek PF3-480-60-01). .... | 11 |
| Figure 14: Electrically heated core ramp up from 0 to 100% duty cycle in 10% increments. Measured electrical power in electrically heated core vs time for the original SSR powered system (top, red) and the SCR powered system (bottom, black) .....  | 12 |
| Figure 15: Electrically heated core ramp up from 0 to 100% duty cycle in 10% increments. Measured electrical power in electrically heated core vs duty cycle for the original SSR powered system (top, red) and the SCR powered system (bottom, black).....   | 13 |
| Figure 16: Isometric drawing of current core insulator design.....  | 14 |
| Figure 17: Boundary conditions for core insulator. Left: thermal boundary condition. Right: mechanical boundary condition. ....   | 15 |
| Figure 18: Equivalent (Von-Mises) stress result .....   | 15 |
| Figure 19: THETA instrumentation port locations.....  | 17 |
| Figure 20: Diagram showing the data acquisition and control infrastructure for THETA.....   | 18 |
| Figure 21: THETA control and data visualization software .....  | 19 |
| Figure 22: Segment of THETA control script file from test # 2022-05-23-03.....  | 20 |

|   |    |
|---|----|
| Figure 23: THETA pump speed and flowrate vs time from test # 2022-05-23-03.....   | 20 |
| Figure 24: Side view of THETA secondary system showing height of secondary components relative to mezzanine and to the top of the primary flange.....   | 21 |
| Figure 25: CAESAR-II software THETA secondary piping model.....   | 22 |
| Figure 26: Secondary flowmeter isometric view (left), view with grating removed to reveal important constituent components (right).....   | 23 |
| Figure 27: Secondary flowmeter surfaces with convection coefficient set to 1 W/m <sup>2</sup> K shown in blue, all other surfaces adiabatic (left). Surface temperature profile with flow pipe temperature set to 670 °C (right). .....   | 23 |
| Figure 28: COMSOL Multiphysics study, cross section looking down flow pipe at the center of the magnet/yoke assembly showing the electric potential and magnetic flux density at a sodium flowrate of 5 GPM .....   | 24 |
| Figure 29: Photo of THETA Secondary permanent magnet flowmeter as received .....  | 24 |
| Figure 30: THETA secondary pump and pump curves .....   | 25 |
| Figure 31: THETA IHX side view.....   | 25 |
| Figure 32: IHX view showing the downcomer/upcomers and baffles .....  | 26 |
| Figure 33: Cross section showing the two thermal expansion bellows and the downcomer vacuum snorkel .....   | 26 |
| Figure 34: THETA secondary loop sodium-to-air heat exchanger.....   | 28 |
| Figure 35: Optical Fiber Capillary Tube Installation. Capillary 1 (red) will house a fiber to capture shell inner wall temperature during operation. Capillary 2 (blue) will house a fiber to capture liquid sodium temperature in the tubes. Capillary 3 (green) will house a fiber to capture the temperature of the outer tube walls ..... | 28 |
| Figure 36: Photograph showing the installation of fiber capillary tube installation on shell side of AHX.....   | 29 |
| Figure 37: Optical fiber installed in capillary tube through 1/16” compression tee.....   | 29 |
| Figure 38: Geometry of axisymmetric finite element analysis to determine fiber in capillary tube time constant .....  | 30 |
| Figure 39: Temperature response of optical fiber to step change in surface temperature of capillary. Mean convective coefficients, $\bar{h}$ , from 500-5000 shown.....   | 30 |
| Figure 40: Photo of the high-pressure air blow for the air-to-sodium heat exchanger. (PN: Cincinnati Fan HP-8D19) .....   | 31 |
| Figure 41: Sodium testing. Temperature (°C) vs distance vs time. Sodium flowrate: 5 GPM. Heater power initially 0%, tripped on at 120 s to 51.4% duty cycle (~20 kWe). Heater tripped to 0% duty cycle at 1120 s. Top IHX outlet window open .....  | 33 |
| Figure 42: Water testing. Normalized temperature (°C) vs distance vs time. water flowrate: 5 GPM. Heater power initially 0%, tripped on at 120 s to 51.4% duty cycle (~20 kWe). Heater tripped to 0% duty cycle at 1120 s. Top IHX outlet window open.....  | 34 |
| Figure 43: Sodium testing. Temperature (°C) vs distance vs time. Sodium flowrate: 5 GPM. Heater power initially 0%, tripped on at 120 s to 51.4% duty cycle (~20 kWe). Heater tripped to 0% duty cycle at 1120 s. Bottom IHX outlet window open.....  | 35 |

Figure 44: Water testing. Normalized temperature (°C) vs distance vs time. Water flowrate: 5 GPM. Heater power initially 0%, tripped on at 120 s to 51.4% duty cycle (~20 kWe). Heater tripped to 0% duty cycle at 1120 s. Bottom IHX outlet window open ..... 36

### LIST OF TABLES

Table 1: THETA instrumentation and measurement. Port positions provided in Figure 19 ..... 16

## 1. Executive Summary

The Thermal Hydraulic Experimental Test Article (THETA) is a facility that is used to develop sodium components and instrumentation as well as acquire experimental data for validation of reactor thermal hydraulic and safety analysis codes. The facility simulates nominal conditions as well as protected/unprotected loss of flow accidents in a sodium-cooled fast reactor (SFR). High fidelity distributed temperature profiles of the developed flow field may be acquired with Rayleigh backscatter based optical fiber temperature sensors. The facility was designed in partnership with systems code experts to tailor the experiment to ensure the most relevant and highest quality data for code validation.

THETA is comprised of a traditional primary and secondary system. The primary system is submerged in the pool of sodium and consists of a pump, electrically heated core, intermediate heat exchanger, and connected piping and thermal barriers (redan). The secondary system, located outside of the sodium pool, consists of a pump, sodium to air heat exchanger, and connected piping and valves. To date the primary system is on line and the secondary system is under construction.

Figure 1 illustrates the main components of the primary system. Figure 2 provides a drawing of the THETA secondary system components. The THETA primary system was installed in the Mechanisms Engineering Test Loop (METL) 28 inch Test Vessel #4, Figure 3. Since the FY21 THETA status report, vessel 4 was filled with sodium for the first time to facilitate commissioning of the THETA primary system components in sodium. The control system for the electrically heated core has been upgraded to provide more linear and predictable performance. Optical fibers have been installed and thermal stratification tests using the primary system have been performed to assess the performance of these sensors.

The secondary system construction is well underway. The secondary system underwent a design modification to raise the elevation of the secondary system as to not conflict with the rest of the testing area within METL. The system was designed to pass ASME B31.3 pipe code for all possible operating scenarios, the design was approved and stamped by a professional piping engineer. The secondary, AC Conduction based electromagnetic pump from CMI Novacast (product number CA-15) was delivered. The custom designed permanent magnet based secondary flowmeter was delivered. The intermediate heat exchanger design is in fabrication and will be delivered before end of calendar year 2022. Note that the intermediate heat exchanger was scheduled for delivery during FY22, however due to staffing and material acquisition issues at the manufacturer, the delivery was delayed.



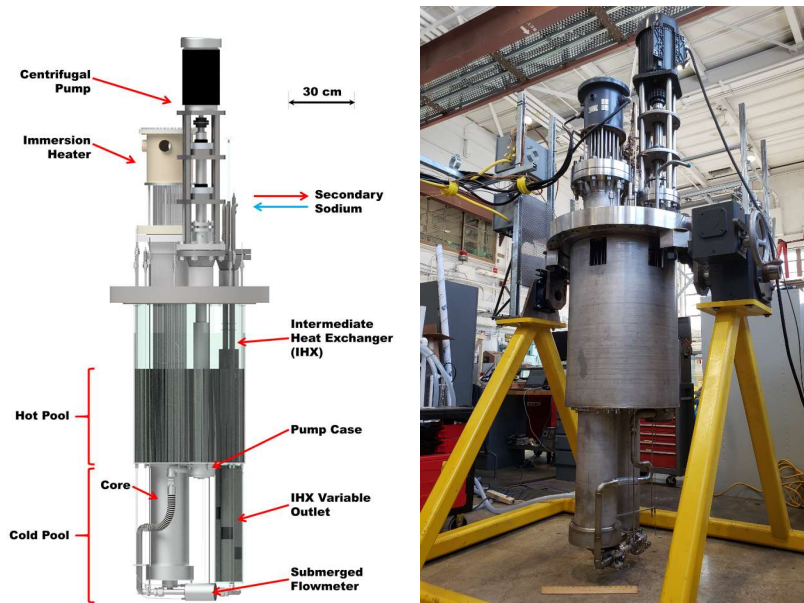


Figure 1: THETA primary system

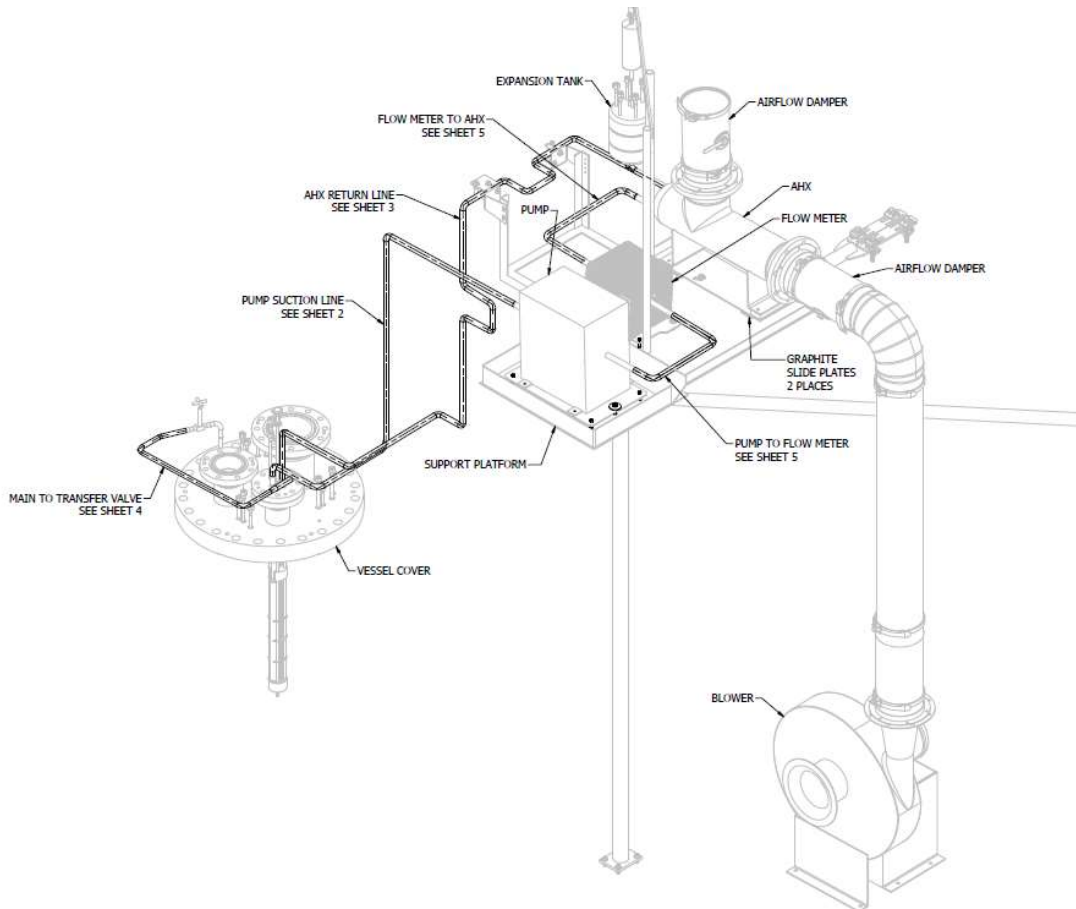


Figure 2: Isometric drawing of THETA secondary system



**Figure 3: THETA installed in METL test vessel #4. Left: uninsulated without pump motor installed. Right: insulated with pump motor installed.**

## 2. Introduction

The Thermal Hydraulic Experimental Test Article (THETA) is a METL vessel experiment designed for testing and validating sodium fast reactor components and phenomena. THETA has been scaled using a non-dimensional Richardson number approach to represent temperature distributions during nominal and loss of flow conditions in a sodium fast reactor (SFR), this analysis was detailed in the THETA FY19 report [1]. The facility is being constructed with versatility in mind, allowing for the installation of various immersion heaters, heat pipes, and heat exchangers without significant facility modification. THETA was designed in collaboration with systems code experts to inform the geometry and sensor placement to acquire the highest value code validation data.

### 2.1. System Overview and Systems Code Application

THETA possesses all the major thermal hydraulic components of a pool type sodium cooled reactor. Figure 4 shows the piping and instrumentation diagram (P&ID) for the primary and secondary sodium circuit. A cross section of the primary vessel shows the pool and core geometry, Figure 5. As can be seen, a 28" METL test vessel is used for the primary sodium "reactor" vessel. An isometric drawing of the secondary sodium system including the piping, pump, flowmeter and air-to-sodium heat exchanger (AHX) can be found in Figure 2.

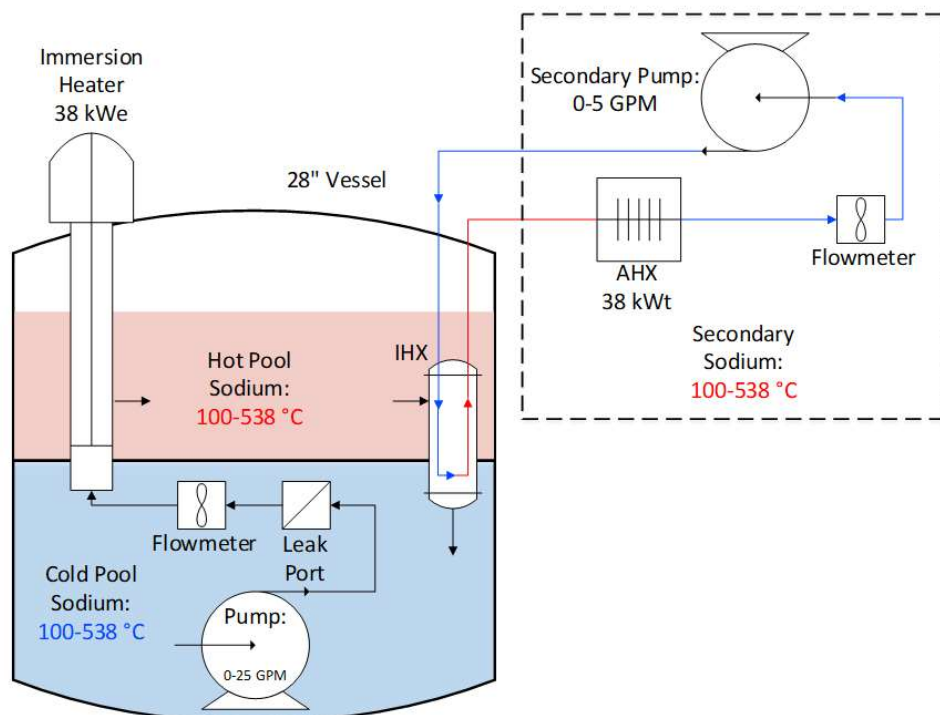
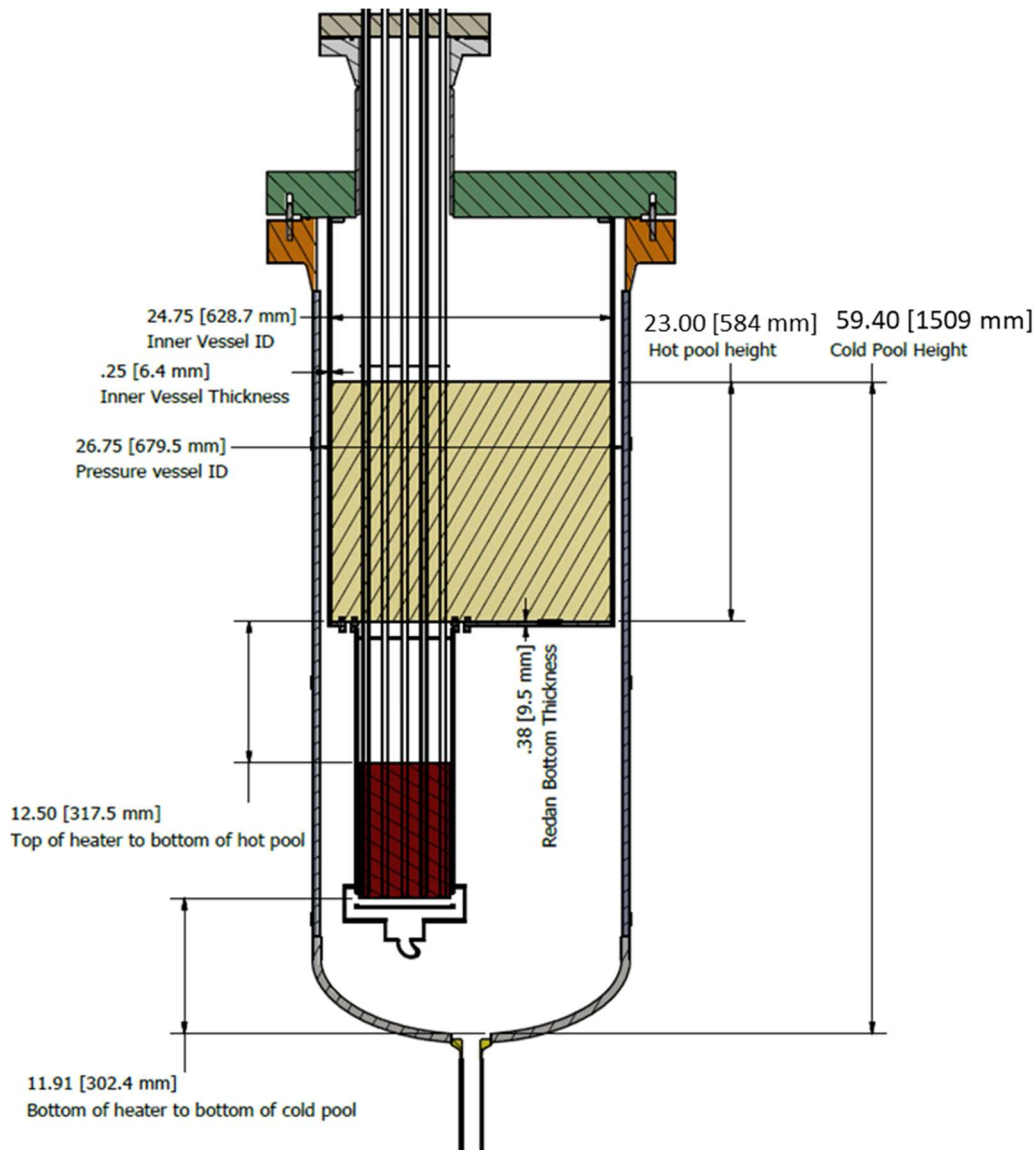
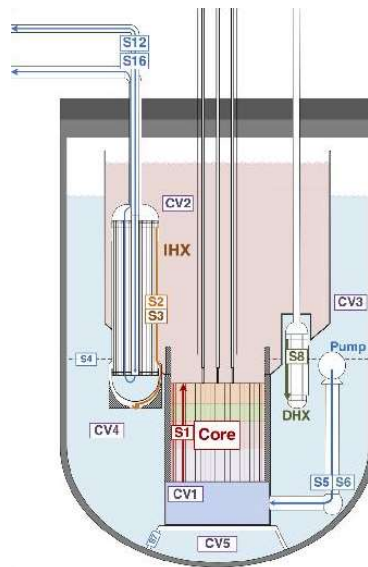


Figure 4: P&ID schematic of THETA



**Figure 5: THETA pool and core geometry. Core nominal diameter: 0.2 [m] (8”), core heated length: 0.3 [m] (12”)**

Argonne National Laboratory’s SAS4A/SASSYS-1 computer code is used for thermal hydraulic and safety analysis of power and flow transients in liquid metal cooled reactors. Figure 6 gives a graphic displaying the segments and compressible volumes used to perform the deterministic analysis of anticipated events such as protected/un-protected loss of flow reactor trips etc. While SAS4A/SASSYS-1 was benchmarked against tests in historic reactors, such as EBR-II [2], a modern liquid metal thermal hydraulic facility is required for further system’s code validation. Please see [1] for an overview of the current systems code modeling efforts as applied to THETA.



**Figure 6: Schematic of SAS4A/SASSYS-1 showing locations of various compressible volumes (CV#) and segments (S#)**

### **3. Primary System Development**

The following section presents a summary of all primary system components as of September 2022 - Figure 1 provides a schematic of the primary system and Figure 7 provides a photo of primary system components for reference. The primary system was tested with deionized water in FY20 and early FY21 at Argonne's Building 206 [3]. The system was then transported to Building 308 where the Mechanisms Engineering Test Loop (METL) is located [4]. The system was disassembled for modifications to improve performance, as informed by the deionized water campaign. The primary system was then sanitized, rinsed and dried for final reassembly. Once reassembled, and all sensors function tested and locations documented, the system was commissioned and installed in the METL 28" test vessel #4. During FY22, METL test vessel #4 was filled with sodium for the first time and commissioning of the THETA primary system began.

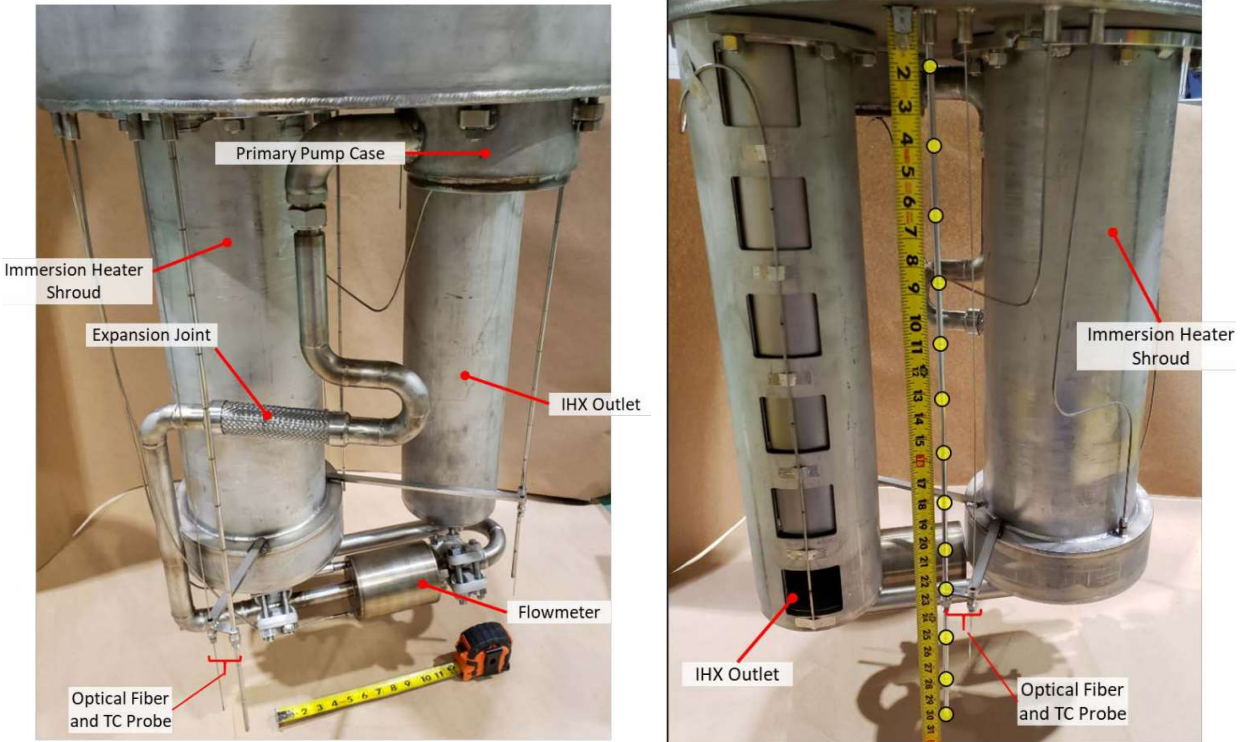


**Figure 7: Photo of THETA primary system cold pool components**

### 3.1. Primary Pump and Flowmeter

The THETA primary pump is a custom built, all stainless steel centrifugal pump. The pump was characterized with deionized water to produce pump curves in [3]. After charging the THETA primary system with sodium, the pump was commissioned in sodium by varying the pump speed from zero to 1,100 RPM in 100 RPM increments over a period of 220 minutes, Figure 8. The flowmeter flowrate as a function of time was plotted for this test in Figure 9. Note that the flowmeter was calibrated in [5], the flowrate was determined from the induced voltage, sodium temperature, and magnet temperature using Eq. 1. All of the terms of Eq. 1 were fully described in [5]. The flowrate as a function of pump speed was plotted in Figure 10. This data was fit to a cubic function demonstrating the relative non-linearity of the pump at low pump speeds compared to higher pump speeds.

$$Q = C \frac{\pi V_m d}{4BK_B K_W K_E} \quad (1)$$

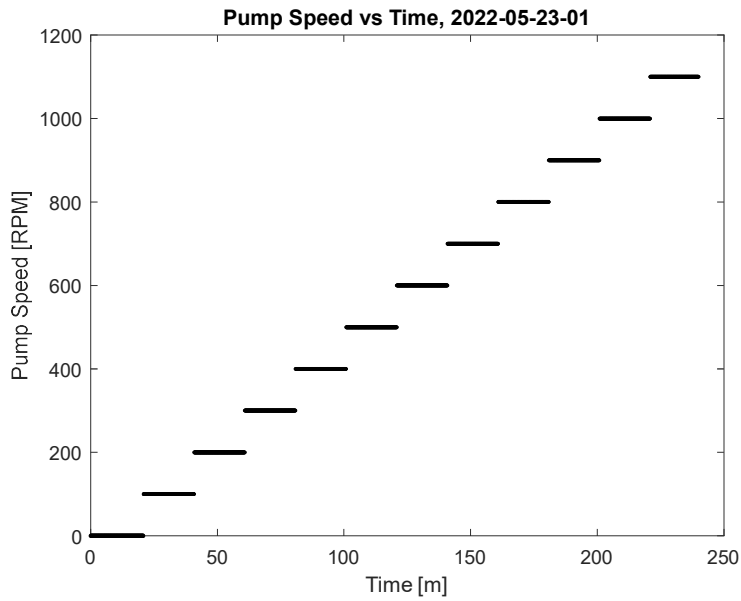


**Figure 8: THETA pump speed vs time during sodium commissioning test # 2022-05-23-01**

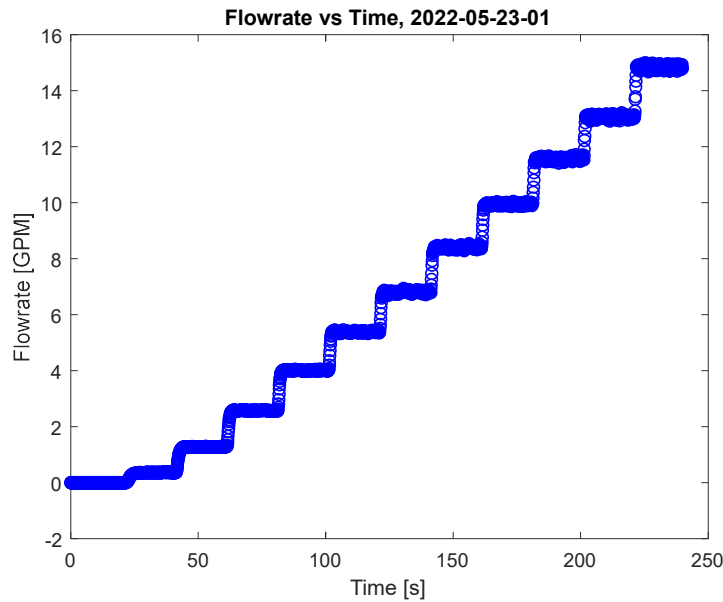


**Figure 9: THETA flowmeter flowrate vs time during sodium commissioning test # 2022-05-23-01. Sodium temperature at pump inlet: 203.1 °C. Flowmeter magnet temperature: 193.1 °C.**

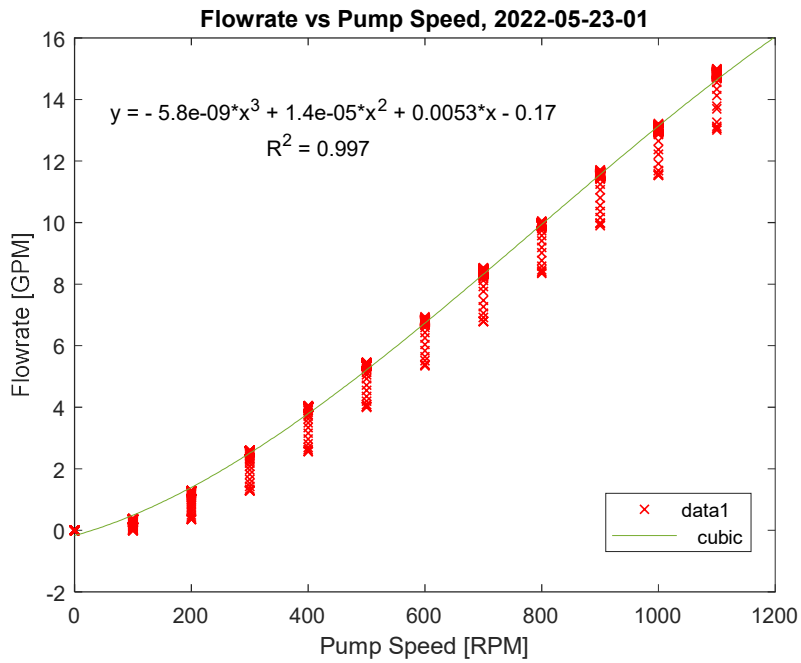


**Figure 10: THETA flowrate vs pump speed during sodium commissioning test # 2022-05-23-01.**

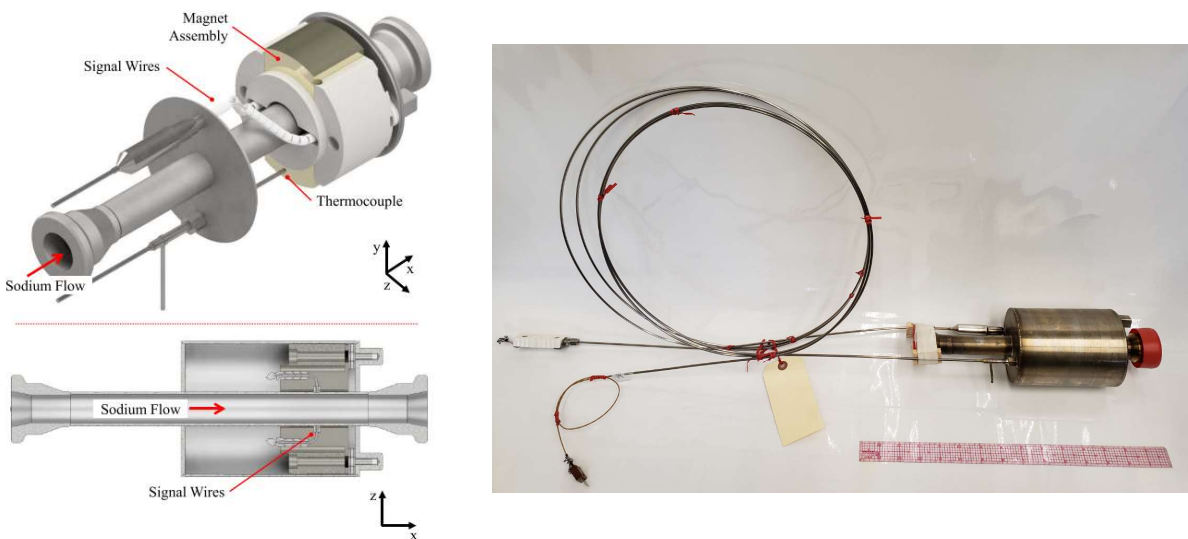


**Figure 11: Photo of completed THETA submersible electromagnetic flowmeter with 15" ruler for reference. Note the 1/8" MI cables transmitting temperature and sensor data have been spooled up for easy transport**



### 3.2. Electrically Heated Core

During FY22 the control panel for the electrically heated core was updated. The manufacturer supplied control system for the 38 kW electrically heated core was driven with a 3 phase SSR relay, Figure 12. While this control system satisfies typical industrial process control requirements such as heating a fluid to a particular temperature and maintaining it within a margin, it does not allow for precise control of heater output power. In order to achieve precise power control to simulate various sodium fast reactor core phenomena a phase angle fired SCR controller was used to replace the SSR controller.

An Ametek three phase SCR power controller was procured (PN: PF3-480-60-01). A custom power enclosure was built at Argonne to house the SCR controller along with the appropriate fuses, a Schneider electric PM5110 power meter, and a dedicated over-temperature relay to shut off the immersion heater at high temperature to protect the heater if the main THETA control program fails, Figure 13.

To demonstrate the performance of the upgraded phase angle fired SCR system an experiment was performed where the duty cycle of the fully sodium submerged electrically heated core was brought from 0-100% duty cycle in 10% increments. This experiment was performed with the original SSR control system and with the upgraded SCR system. Figure 14 presents the measured electrical power vs time during ramp up from 0-100% duty cycle for both the SSR and SCR controlled systems. As can be seen the SCR system produces more even and predictable power with minimal noise. The measured power vs duty cycle has been plotted for these two control systems in Figure 15. As can be seen the SSR system possesses a knee in electrical power at 40% duty cycle whereas the SCR system has a linear power profile across the entire duty cycle with a linear function fit to the data with an R-squared value of 0.978 (linear function included in the plot).

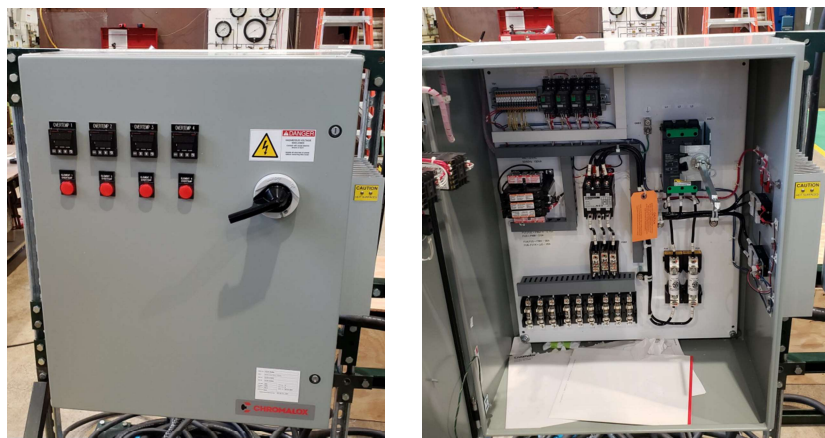


**Figure 12: Manufacturer supplied SSR panel**

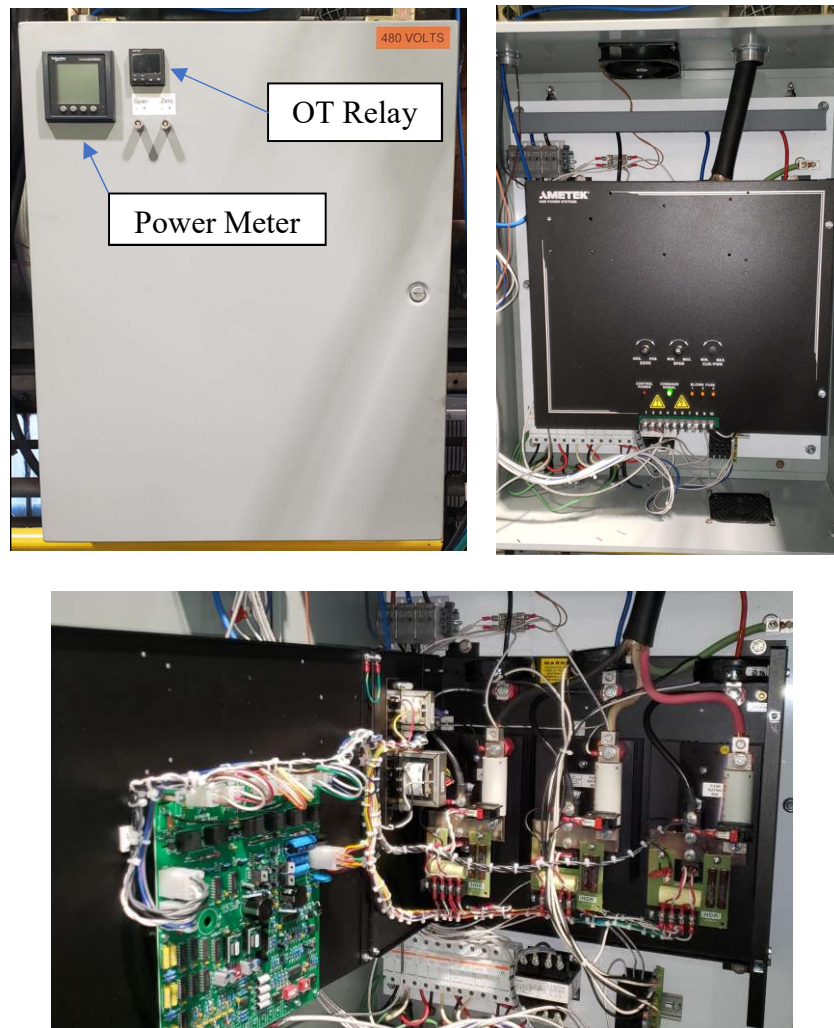


**Figure 13: Updated control panel for electrically heated core using phase angle fired SCR control. Top left shows the outside of the enclosure where the Schneider electric PM5110 power meter and dedicated over temperature controller are located. Top right shows the inside of the enclosure. Bottom shows the internals of the three phase SCR (PN: Ametek PF3-480-60-01).**

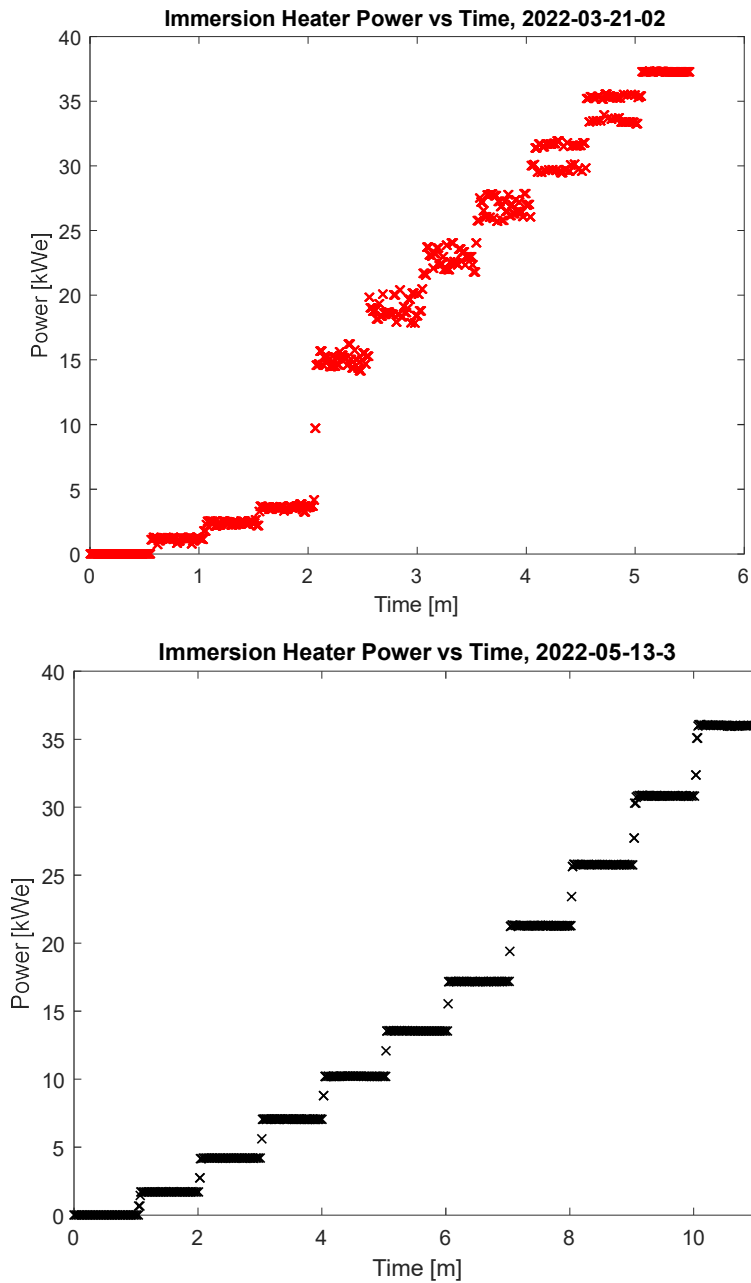


**Figure 14: Electrically heated core ramp up from 0 to 100% duty cycle in 10% increments. Measured electrical power in electrically heated core vs time for the original SSR powered system (top, red) and the SCR powered system (bottom, black)**

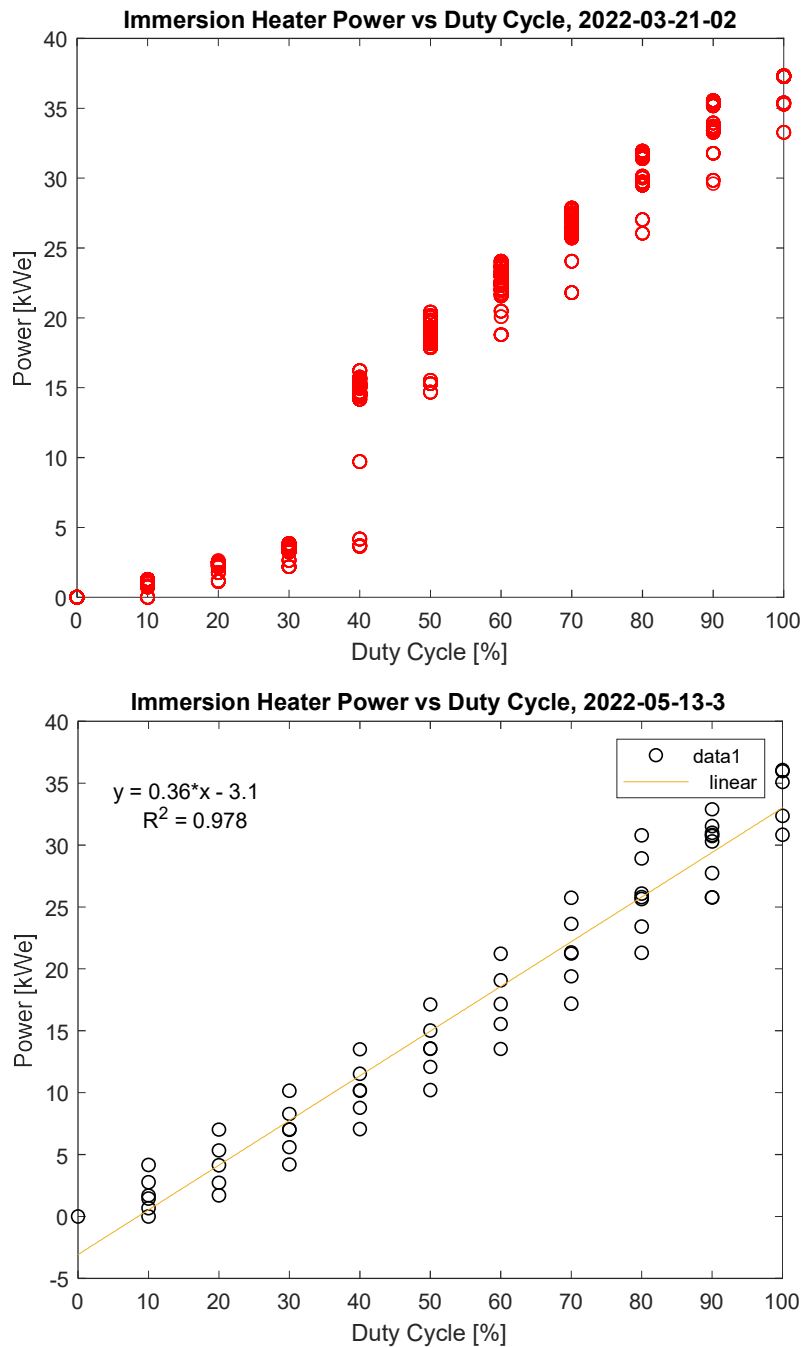


**Figure 15: Electrically heated core ramp up from 0 to 100% duty cycle in 10% increments. Measured electrical power in electrically heated core vs duty cycle for the original SSR powered system (top, red) and the SCR powered system (bottom, black)**

Systems code engineers at ANL have performed qualitative initial analyses of experimental THETA data acquired with the immersion heater activated. The thermal conductivity from the electrically heated core to the cold pool of THETA may be too high – to the point where scaling the thermal hydraulic data to a full size SFR may not be feasible. Therefore, it was recommended that a thermal insulator be designed that may be installed over the 8.63” outer diameter electrically heated core shroud. This insulator would consist of two clamshell pieces that could be installed without major disassembly of the existing primary system. The insulator would ideally be able to be installed while THETA was in the Flexicask system [6] to eliminate the requirement to expose THETA to atmosphere so that removing sodium residue from the entire test article would not be required. An isometric drawing of the current insulator design can be found in Figure 16. This insulator is designed with 16 gauge Inconel 718. There is an annular gap created that can be filled with low thermal conductivity inert gas or a vacuum pulled for maximum thermal insulation.

When the insulator is installed over the electrically heated core shroud and the heater is on there will be a significant differential temperature between the inner and outer diameter of the insulator. In addition, the assembly will also have a pressure head imposed on the material if the insulator is under vacuum and there exists a sodium and argon pressure head. Therefore, an ANSYS finite element analysis was performed to assess the maximum stress on the structure.

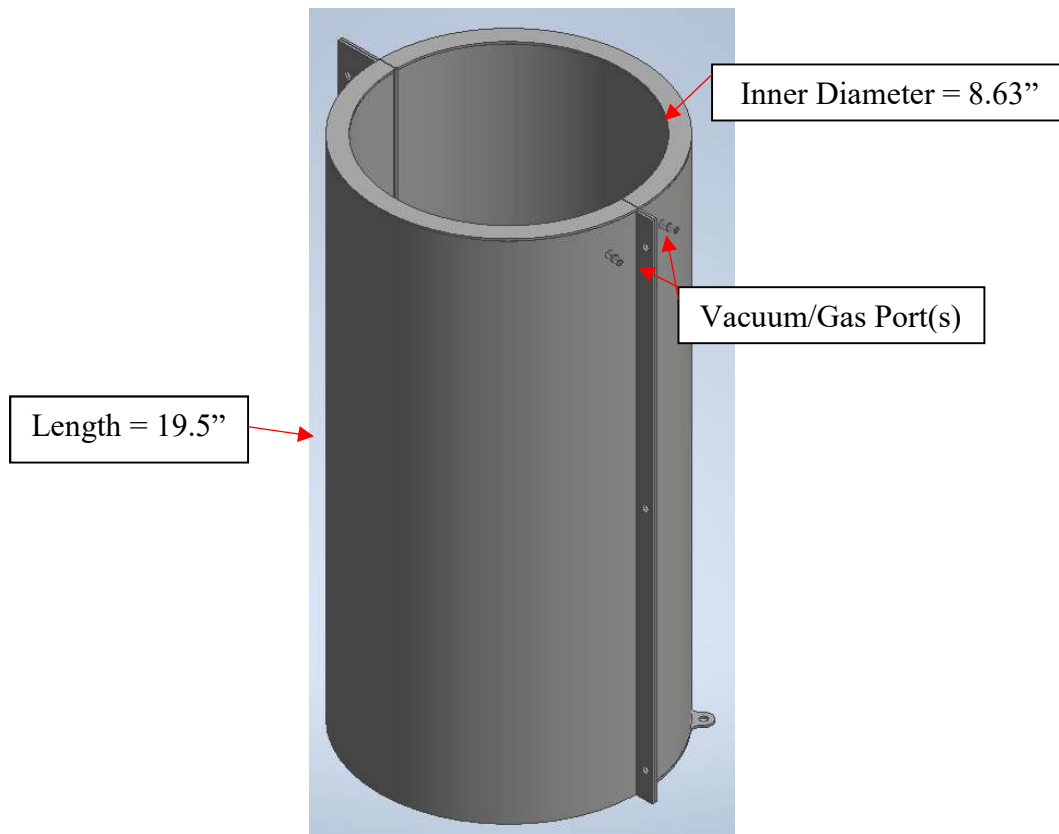


**Figure 16: Isometric drawing of current core insulator design**

Figure 17 provides the boundary conditions applied to the core insulator. A thermal analysis was first performed to determine the temperature distribution in the assembly with a 300 °C constant temperature applied to the inner diameter and a 400 °C constant temperature applied to the outer diameter. The temperature distribution from this analysis was then linked to a structural analysis. A pressure of  $1.72 \times 10^5$  Pa (25 PSI) was applied to the outer surface of the structure to simulate vacuum and a sodium/argon pressure head. The maximum Von-Mises equivalent stress determined was 553 MPa, Figure 18.

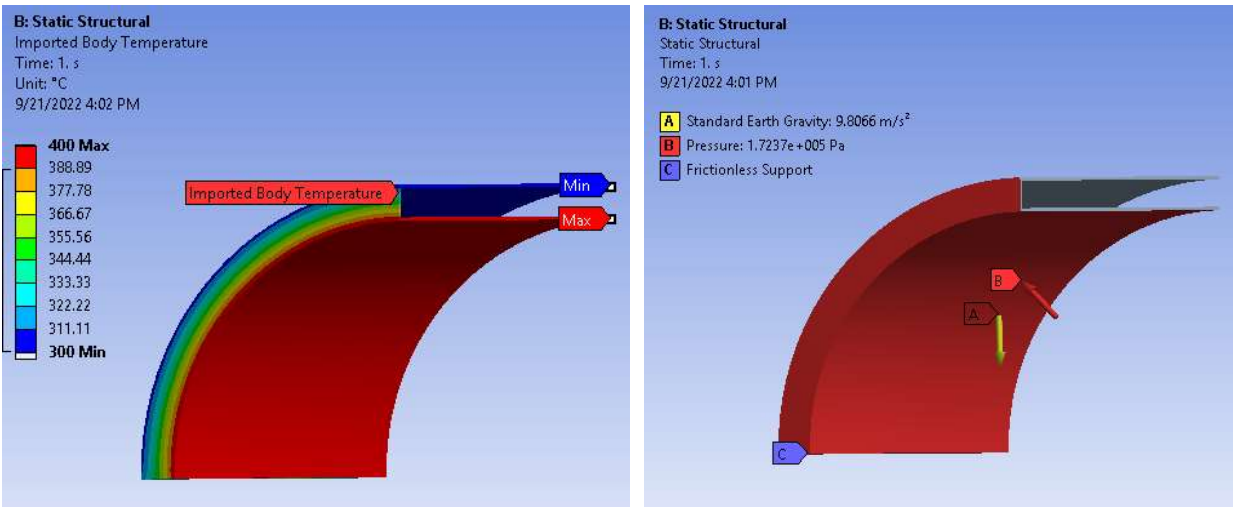


**Figure 17: Boundary conditions for core insulator. Left: thermal boundary condition. Right: mechanical boundary condition.**

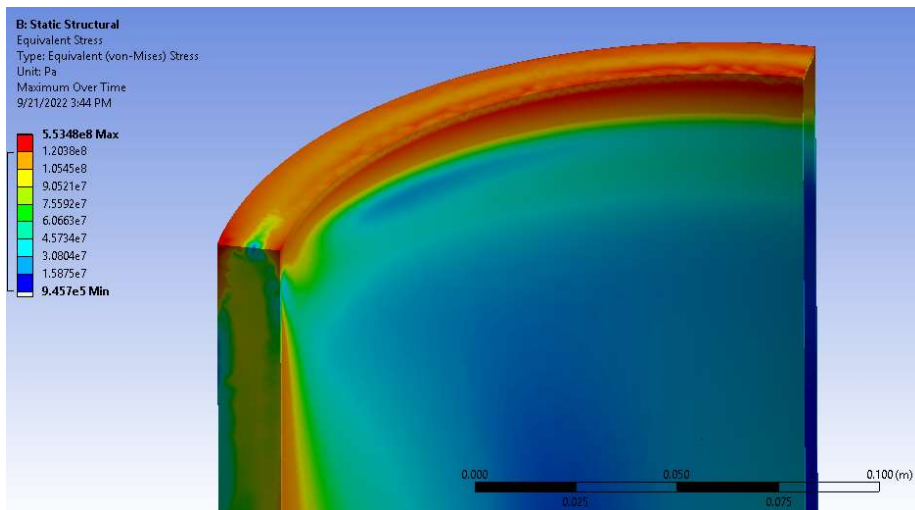


**Figure 18: Equivalent (Von-Mises) stress result**

### 3.3.Data Acquisition and Control

Table 1 summarizes THETA instrumentation that includes single and multi-point thermocouples, distributed optical fiber temperature sensors, level sensor, and flowmeter voltage measurements. The port locations on the top flange have been labeled in Figure 19.

**Table 1: THETA instrumentation and measurement. Port positions provided in Figure 19**

| Port  | Instrument   | Measurement                                       |
|-------|--------------|---|
| 1a    | Single TC    | Pump inlet temperature                            |
| 1b    | Single TC    | Core inlet temperature                            |
| 1c    | Blank        | -   |
| 1d    | Blank        | -   |
| 2     | Single TC    | Core outlet temperature                           |
| 3     | Fiber        | Hot and cold pool distributed axial temperature   |
| 4     | Rake TC      | Hot and cold pool distributed axial temperature   |
| 5a    | Rake TC      | IHX outlet and inner vessel near wall temperature |
| 5b    | Single TC    | Pump shaft column overflow temperature            |
| 5c    | Blank        | -   |
| 5d    | Blank        | -   |
| 6     | Rake TC      | Hot and cold pool distributed axial temperature   |
| 7     | Fiber        | Hot and cold pool distributed axial temperature   |
| 8     | Rake TC      | Inner vessel near wall temperature in cold pool   |
| 9     | Rake TC      | Hot and cold pool distributed axial temperature   |
| 10    | Fiber        | Hot and cold pool distributed axial temperature   |
| 11    | Level Sensor | Sodium hot pool at 23" in elevation               |
| 12a   | MI Cable     | Flowmeter voltage                                 |
| 12b   | Single TC    | Flowmeter temperature                             |
| 12c   | Blank        | -   |
| 12d   | Blank        | -   |
| 13    | Fiber        | Hot and cold pool distributed axial temperature   |
| 14    | Fiber        | IHX distributed axial temperature                 |
| 15    | Rake TC      | IHX distributed axial temperature                 |
| 16-20 | Single TCs   | Core temperature 3" above bottom of elements      |

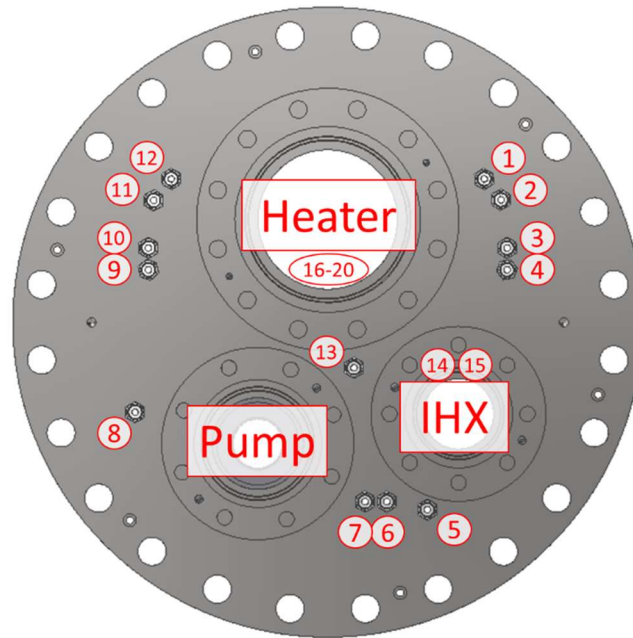


**Figure 19: THETA instrumentation port locations**

A diagram has been provided in Figure 20 illustrating the data acquisition and control scheme for the THETA primary system. As can be seen a THETA Control PC serves as the central control system for THETA. A National Instruments (NI) CompactRIO 9035 Controller and NI 9149 expansion chassis acquire thermocouple data using NI 9212 cards. The NI 9212 are 8-channel temperature input modules that offer channel-to-channel isolation to optimize the signal to noise ratio. An NI 9266 module controls the primary pump and electrically heated core process outputs via a 4-20 mA current loop. An NI 9476 module provides a 5VDC signal to turn the primary pump and/or electrically heated core on/off and triggers a 5V TTL signal to synchronize the optical fiber data acquisition with the rest of the system. An NI 9207 module acquires sodium level from the point level sensor [4]. The NI CompactRIO chassis acquires power data from the electrically heated core with Modbus TCP/IP protocol from a Schneider Electric PM5110 power meter. The THETA Control PC communicates with METL infrastructure via Modbus TCP/IP to acquire METL vessel 4 information (argon pressure, heater power, process temperature).



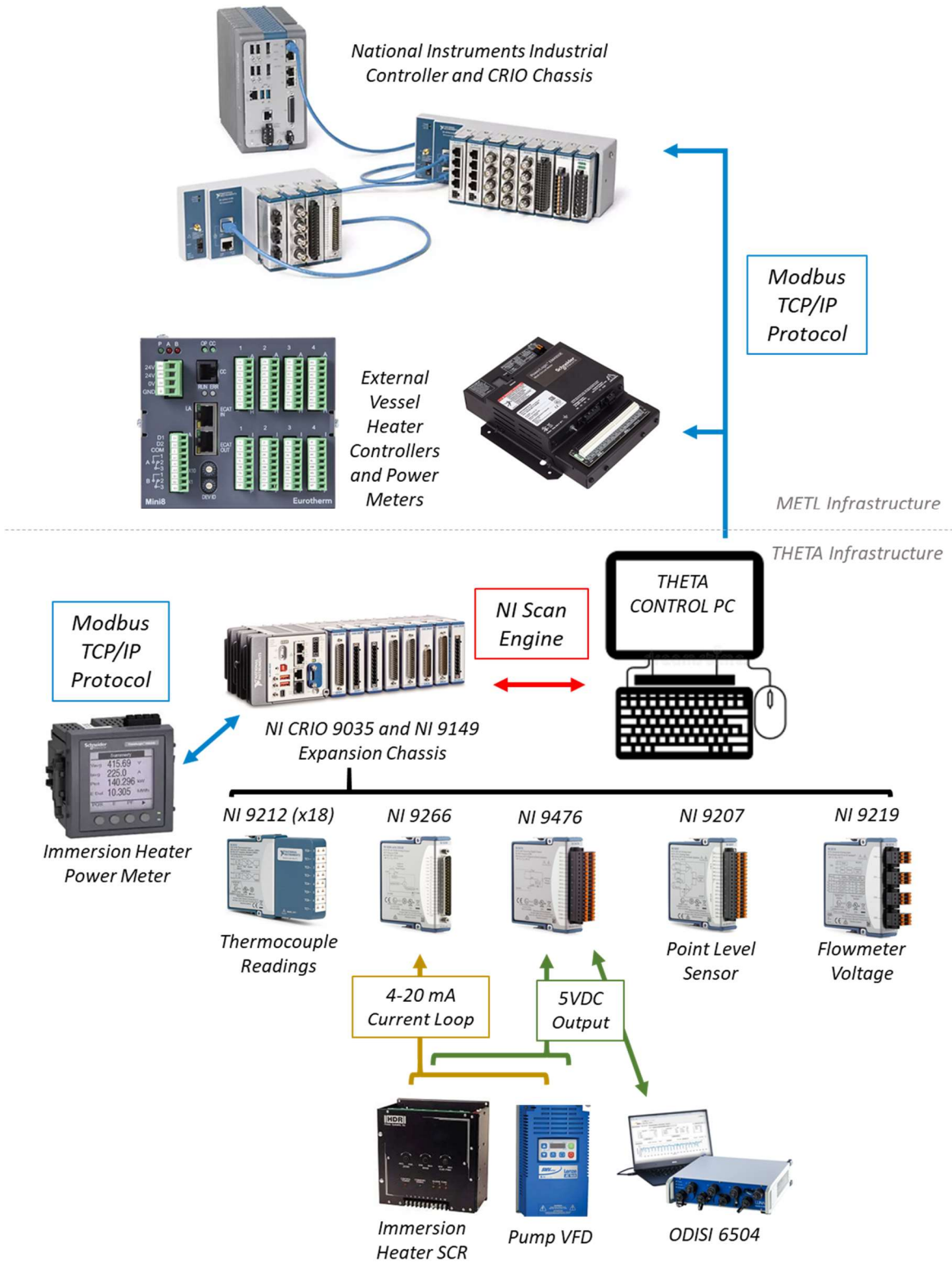


**Figure 20: Diagram showing the data acquisition and control infrastructure for THETA**

A screengrab of the custom THETA software can be found in Figure 21. The software, written in Labview 2018, allows the user to control all system components and view all system parameters.

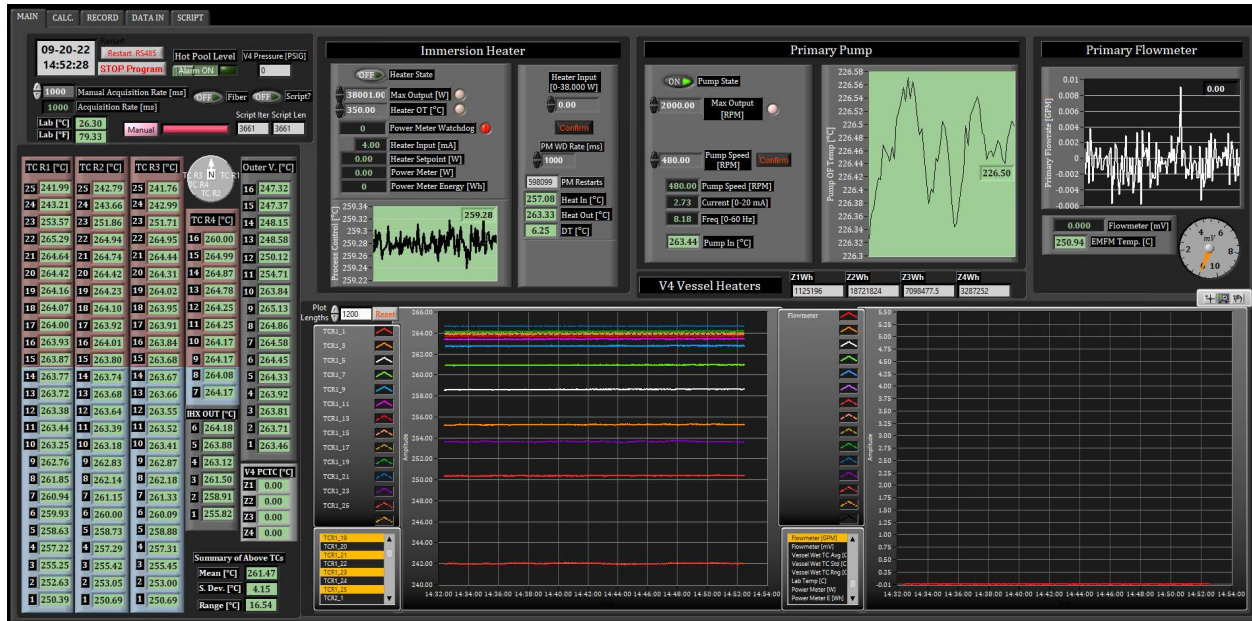


Figure 21: THETA control and data visualization software

A feature was added to the THETA control system to use a script to control system parameters. This was implemented in order to reduce the amount of user intervention and facilitate advanced control profiles for the heater, pump, etc. An example of a script that was implemented by THETA control can be found in Figure 22. This test reduced the pump output speed exponentially from 950 RPM to simulate a pump spin down during a reactor trip. Figure 23 provides the normalized pump speed and flowrate as a function of time for this test.

The current script program takes as inputs: start time of test, data acquisition time, control resolution (how fast a parameter may change), heater duty cycle, and pump speed. The script program will be expanded to control secondary parameters when the secondary system is brought online.

| Start Time [HH:MM:SS<br>mm/dd/yyyy] | Acquisition Rate<br>[ms] | Control<br>Resolution | Time [s] | Heat<br>Duty [%] | Speed<br>[RPM] |
|-------------------------------------|--------------------------|-----------------------|----------|------------------|----------------|
| 5/23/2022 15:57                     | 100                      | 10                    | 0        | 0                | 950            |
|                                     |                          |                       | 1        | 0                | 946.3316       |
|                                     |                          |                       | 2        | 0                | 942.6632       |
|                                     |                          |                       | 3        | 0                | 938.9948       |
|                                     |                          |                       | 4        | 0                | 935.3264       |
|                                     |                          |                       | 5        | 0                | 931.658        |
|                                     |                          |                       | 6        | 0                | 927.9896       |
|                                     |                          |                       | 7        | 0                | 924.3212       |
|                                     |                          |                       | 8        | 0                | 920.6528       |
|                                     |                          |                       | 9        | 0                | 916.9844       |
|                                     |                          |                       | 10       | 0                | 913.316        |
|                                     |                          |                       | 11       | 0                | 909.6476       |
|                                     |                          |                       | 12       | 0                | 905.9792       |
|                                     |                          |                       | 13       | 0                | 902.3108       |
|                                     |                          |                       | 14       | 0                | 898.6424       |
|                                     |                          |                       | 15       | 0                | 894.974        |

Figure 22: Segment of THETA control script file from test # 2022-05-23-03

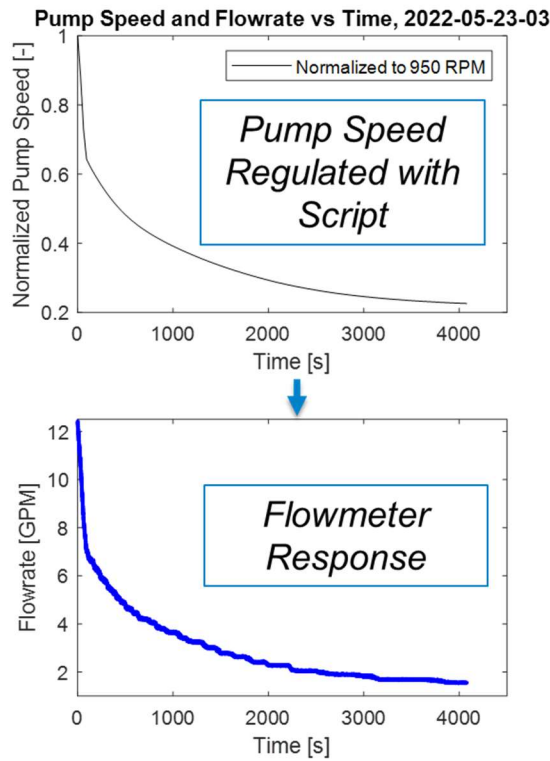
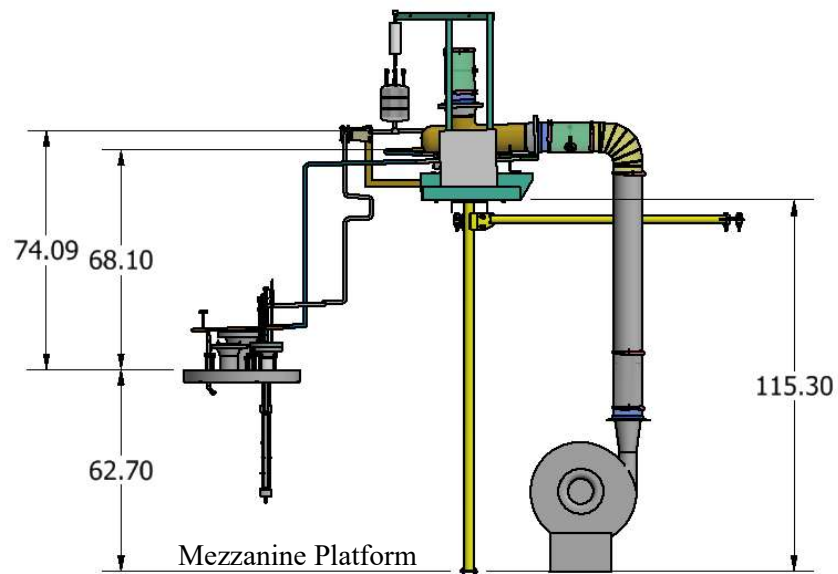


Figure 23: THETA pump speed and flowrate vs time from test # 2022-05-23-03

## 4. Secondary System

### 4.1. Piping Design

In order to preserve area for experimental work on the METL mezzanine the secondary THETA piping was updated this fiscal year from the design previously reported in [4]. An isometric drawing view of the piping network was given in Figure 2. As can be seen in Figure 24, the components of the secondary system were positioned on a platform 115.3” (9.6 feet) off the mezzanine platform. The AHX inlet/outlet nozzles are now positioned at approximately 74” and 68” from the top of the primary flange.



**Figure 24: Side view of THETA secondary system showing height of secondary components relative to mezzanine and to the top of the primary flange.**

The updated piping was analyzed with CAESAR II piping software to ensure the piping network passed ASME B31.3 piping code under any possible operating condition. The analysis was stamped by a qualified professional engineer from J.E. Hodgson Consulting. A picture of the secondary piping network in CAESAR-II can be found in Figure 25.

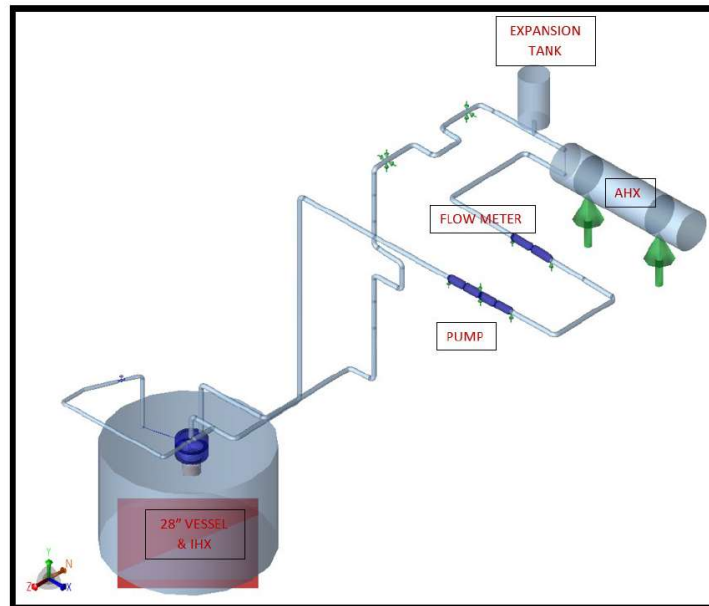


**Figure 25: CAESAR-II software THETA secondary piping model**

#### **4.2.Secondary Flowmeter**

A permanent magnet flowmeter was designed to acquire sodium flow rate in the THETA secondary loop, Figure 26. The sodium flows through a 3/4" SCH 40 stainless steel pipe where a magnetic field interacts with the flowing sodium to produce a voltage signal. A thermal analysis study was performed on the flowmeter where the flow pipe was set to a temperature of 670 °C and the surface temperature of the flowmeter components were characterized Figure 27. It is important that the magnet temperature stay near room temperature, especially for powerful Neodymium magnets which possess a maximum operating temperature of ~80°C. A preliminary magnetohydrodynamic finite element analysis was run to assess the induced voltage of the flowmeter at a nominal 5 GPM flowrate, Figure 28. A signal of 3.4 mV is predicted at 5 GPM.

A photo of the as received secondary permanent magnet flowmeter can be found in Figure 29.

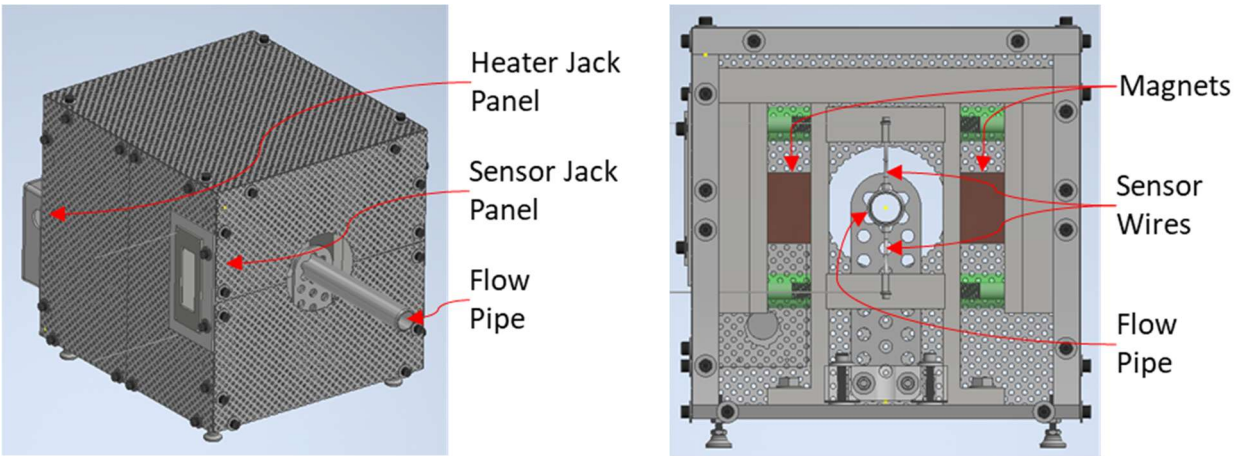


**Figure 26: Secondary flowmeter isometric view (left), view with grating removed to reveal important constituent components (right)**

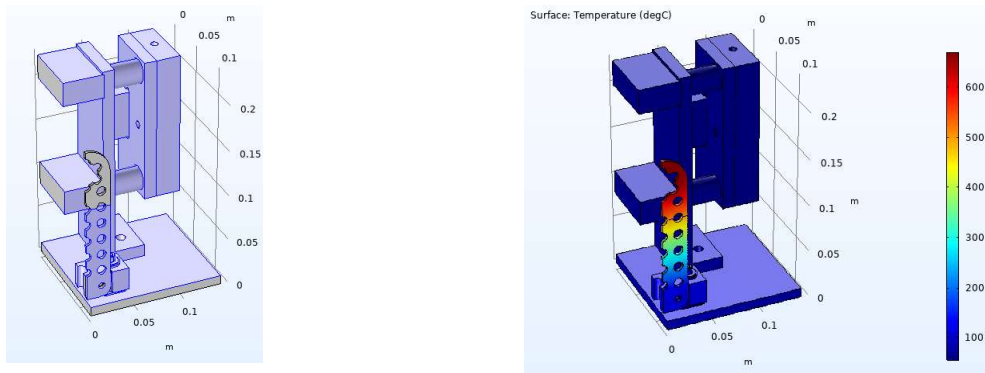


**Figure 27: Secondary flowmeter surfaces with convection coefficient set to 1 W/m<sup>2</sup>K shown in blue, all other surfaces adiabatic (left). Surface temperature profile with flow pipe temperature set to 670 °C (right).**

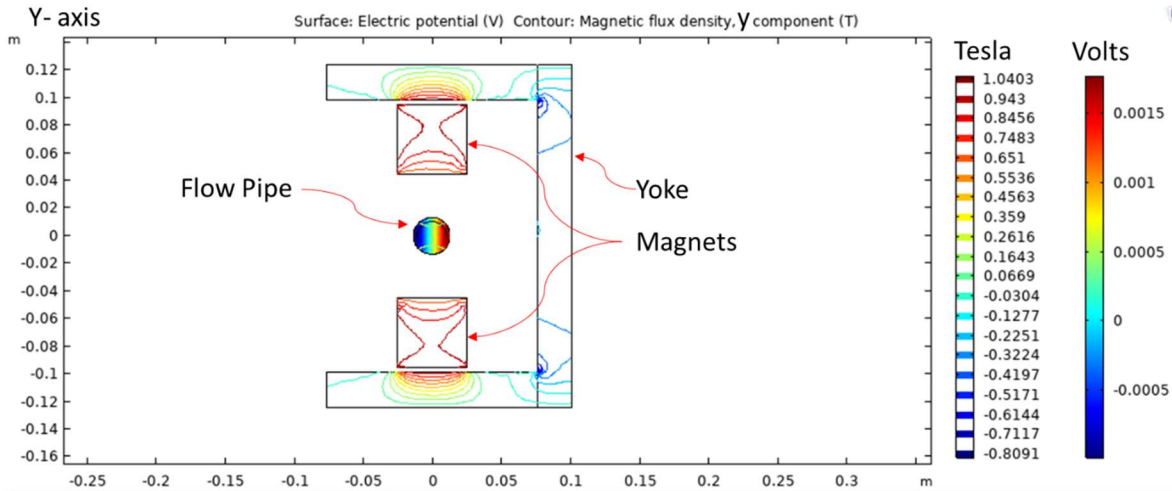


**Figure 28: COMSOL Multiphysics study, cross section looking down flow pipe at the center of the magnet/yoke assembly showing the electric potential and magnetic flux density at a sodium flowrate of 5 GPM**

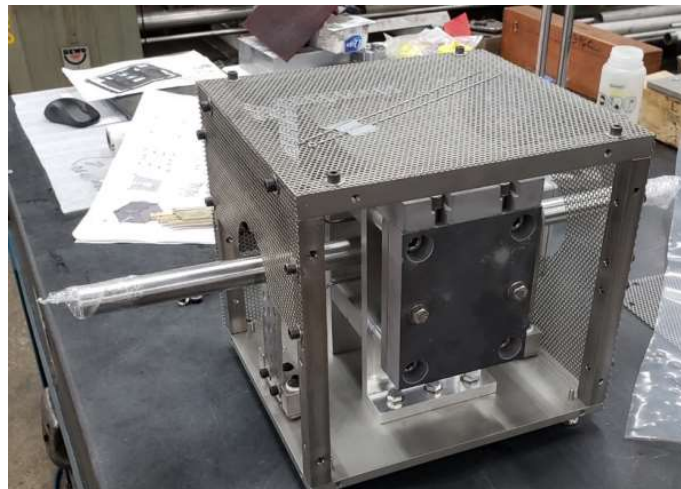


**Figure 29: Photo of THETA Secondary permanent magnet flowmeter as received**

### 4.3. Secondary Pump

An AC conduction pump was ordered for the THETA secondary loop (PN: CMI-Novacast CA-15). A photo of a CA-15 pump and the pump curves can be found in Figure 30. The pump was delivered and is ready for installation.

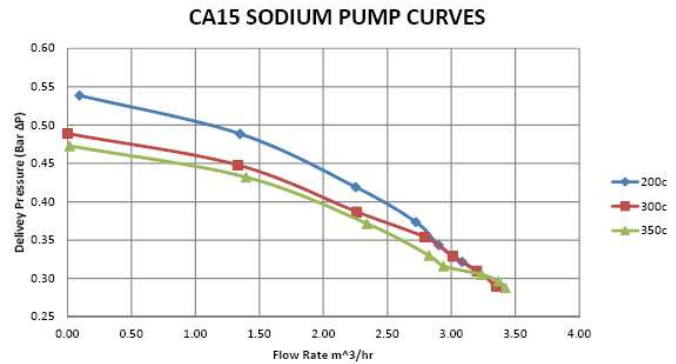


**Figure 30: THETA secondary pump and pump curves**

#### 4.4. Intermediate Heat Exchanger

A design for the intermediate heat exchanger (IHX) was finalized, machine drawings produced, and the assembly was ordered from Ability Engineering Technology in South Holland, IL, Figure 31. Delivery of the IHX is expected end of calendar year 2022.

The IHX possesses a vacuum insulated downcomer to better represent the counter flow heat exchange in a typical SFR, where a large downcomer transports sodium to the bottom of the exchanger in the hot pool, limiting the amount of heat exchange. Then, the sodium flows up through a number of upcomer tubes where the surface area, and thus the heat exchange, is enhanced, Figure 32. In order to reduce the heat exchange in the downcomer tube, it is double walled, whereby a vacuum is able to be pulled in the annular region between the walls with a snorkel that extends from the top of the downcomer to the top of the heat exchanger flange, snorkel shown in green in Figure 33. Given the walls of the downcomer and upcomers will be at different temperatures, given the differential in heat exchange, a pair of thermal expansion bellows will serve to relieve thermal stress, Figure 32 and Figure 33.

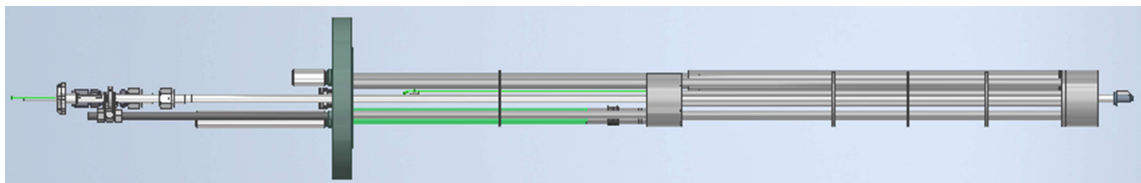


**Figure 31: THETA IHX side view**



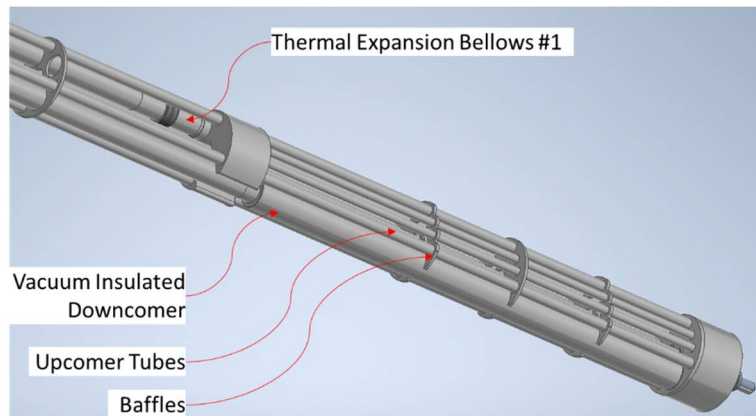


**Figure 32: IHX view showing the downcomer/upcomers and baffles**

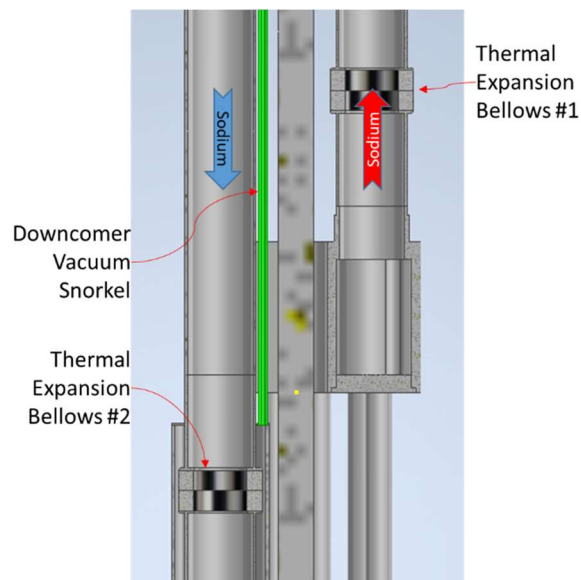


**Figure 33: Cross section showing the two thermal expansion bellows and the downcomer vacuum snorkel**

#### 4.5. Sodium to Air Heat Exchanger

In order to instrument the sodium-to-air heat exchanger in the secondary system with optical fibers, stainless steel capillary tubes were installed in the liquid sodium-to-air shell and tube heat exchanger, Figure 34-Figure 35. These capillary tubes are 316 stainless steel with an outer diameter of 1651  $\mu\text{m}$  (0.065”) and an inner diameter of 1190  $\mu\text{m}$  (0.047”). These capillary tubes are used to:

1. Protect the relatively fragile 150  $\mu\text{m}$  diameter silica single mode optical fibers from hostile environments present in the heat exchanger (liquid sodium and turbulent, high velocity air)

2. Provide a hermetic environment to accommodate a dry, inert cover gas to preserve the optical fibers (reduce moisture induced stress-corrosion attack) [7]
3. Accommodate free thermal expansion of the fibers inside the capillaries to eliminate temperature acquisition errors due to mechanical strain

The capillary tubes were installed in the shell side of the heat exchanger in two locations: on the inner wall of the shell and on the outer wall of the tubes, Figure 35. A capillary tube was also run through the tube side of the heat exchanger. A dual pulse capacitive discharge spot welder was used to weld tabs onto the inner wall of the shell to affix one of the capillary tubes, Figure 36. A 1/16" compression tee fitting was used to facilitate a hermetic seal with gas backfill, Figure 37.

In order to assess the time response of the optical fibers as installed in the capillary tubes, a transient axisymmetric finite element analysis was performed on the geometry using COMSOL Multiphysics, Figure 38. A convective boundary condition varying from 0.5-5 kW/m<sup>2</sup>K was placed on the surface of the capillary tube, a convection coefficient of ~5 kW/m<sup>2</sup>K is typical for liquid sodium flowing in a heat exchanger. [8] A time constant, defined as the amount of time it takes for a sensor to register 63.2% of a step change in temperature, was found for a fiber concentrically located inside of the aforementioned capillary geometry with a helium gas backfill.

Results for the time constant analysis can be found in Figure 39. As can be seen, the time constant of the sensor assembly when the convection coefficient is set to 5,000 W/m<sup>2</sup>K (flowing sodium) is 275 ms. Conversely, when the convection coefficient is set to 500 W/m<sup>2</sup>K (turbulent air) the time constant is 1.83 s. Note that this is the longest possible time constant for the assembly- if the fiber is not perfectly concentric but is resting on the inner wall of the capillary tube the time constant will be reduced. This time response will provide adequate temporal resolution for distributed temperature measurement on the air and sodium side for the phenomena of interest (natural and forced convection flow behavior through the AHX).

The AHX high-pressure air blower (PN: Cincinnati Fan HP-8D19) was delivered and is ready for installation, Figure 40.



Figure 34: THETA secondary loop sodium-to-air heat exchanger

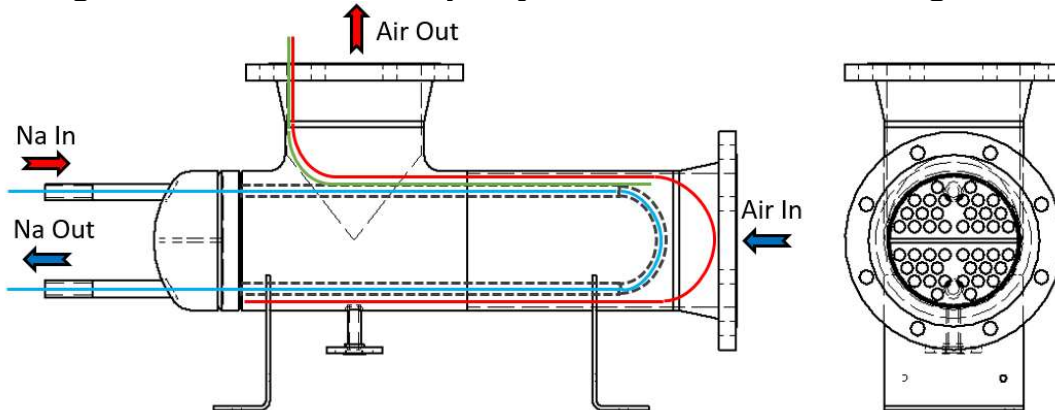
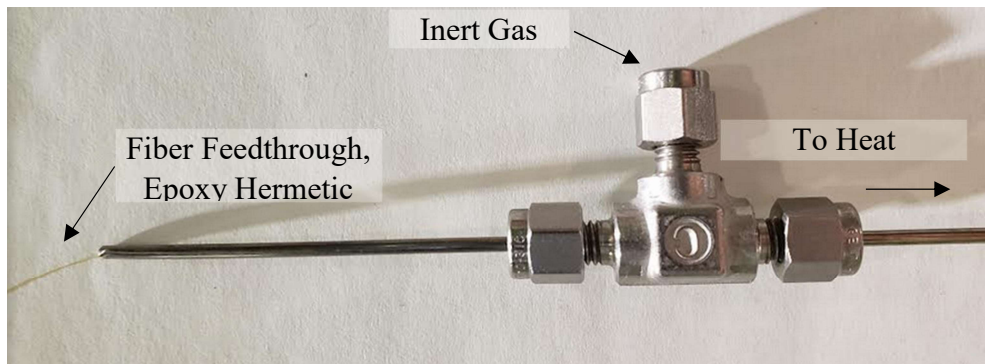


Figure 35: Optical Fiber Capillary Tube Installation. Capillary 1 (red) will house a fiber to capture shell inner wall temperature during operation. Capillary 2 (blue) will house a fiber to capture liquid sodium temperature in the tubes. Capillary 3 (green) will house a fiber to capture the temperature of the outer tube walls



**Figure 36: Photograph showing the installation of fiber capillary tube installation on shell side of AHX**



**Figure 37: Optical fiber installed in capillary tube through 1/16" compression tee.**

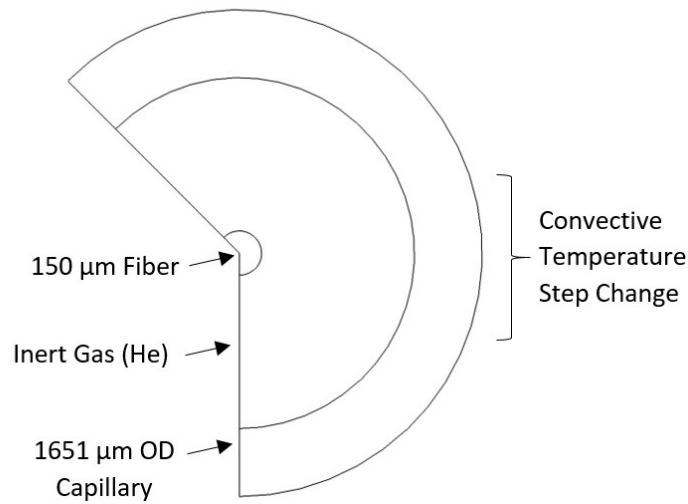


**Figure 38: Geometry of axisymmetric finite element analysis to determine fiber in capillary tube time constant**

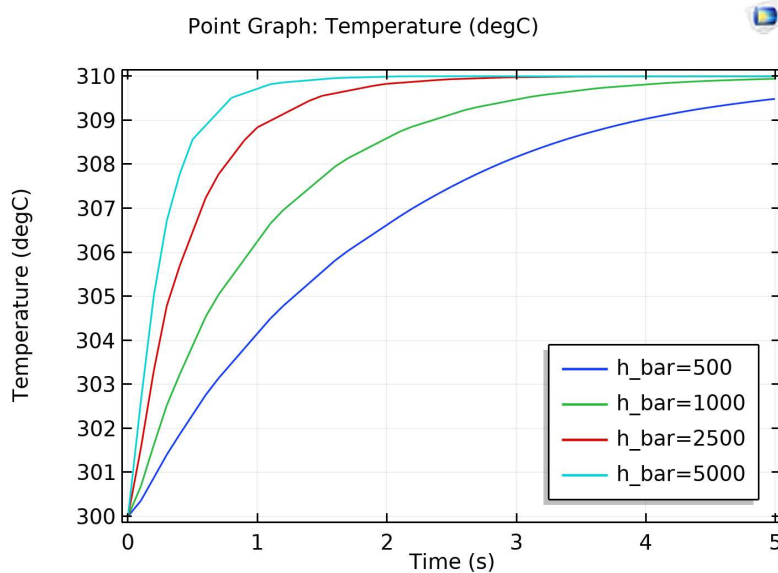


**Figure 39: Temperature response of optical fiber to step change in surface temperature of capillary. Mean convective coefficients,  $h_{\text{bar}}$ , from 500-5000 shown.**



**Figure 40: Photo of the high-pressure air blow for the air-to-sodium heat exchanger.  
(PN: Cincinnati Fan HP-8D19)**

## 5. Experimental Data Generation

Deployment of a sustained advanced reactor pipeline in the U.S. requires that domestic nuclear vendors have the tools necessary to design, analyze, and license reactors with adequate plant safety through a range of possible scenarios. One approach to the analysis and licensing of advanced reactor technologies is the use of systems-level safety analysis codes. While many of these safety analysis codes have undergone decades of development and benchmarking efforts across a range of phenomena, the usage of these codes can greatly benefit from improved modeling of specific phenomena of interest to the domestic nuclear industry.

While a series of historical facilities, both domestic (EBR-II, FFTF, etc.) and international (MONJU, Phénix, etc.), have operated to provide a foundation in prototypic liquid metal fast reactor nominal and transient behavior - including dedicated experiments to understand these phenomena - significant gaps exist in the validation database available for licensing support. In fact, the data generated during these experiments often does not offer sufficient resolution, sensor position quality, or experimental uncertainty quantification. In some cases, data preservation or experimental documentation is inadequate.

THETA presents a unique experimental capability in that its scaling and geometry characteristics are prototypical of the temperature distributions in pool-type SFR designs prevalent in the domestic SFR industry space. The test article includes components for a primary pool (including

hot/cold pools, pump, IHX, and electric core simulant heater) and a secondary sodium heat rejection loop which utilizes a sodium-to-air heat exchanger. Additionally, THETA has been designed to be highly customizable in that alternative components (heat pipes, heat exchangers, etc.) can be inserted into the test article. These characteristics make THETA a great facility for advanced reactor vendors licensing support.

To this end, a GAIN voucher has been awarded by the DOE to Oklo Inc. in partnership with Argonne (CRADA 2021-21121). The project seeks to address two specific phenomena of interest to thermal-hydraulic behavior in liquid metal fast reactors: thermal stratification and transition to natural circulation. Oklo is partnering with Argonne National Laboratory to conduct an experimental investigation into these two phenomena. A complete experimental matrix has been developed in conjunction with the thermal-hydraulic experts at Argonne and the key experimental steps to be performed are described below:

1. Starting from a steady-state forced convection flow in the primary and/or secondary systems to a pump-off state.
2. Starting from pump-off state in primary and/or secondary systems, execute a test matrix of heater (core) power profiles to study the transition to natural circulation.

During these experiments, well-pedigreed data is being generated, modern sodium-based experimental testing methods and data uncertainty quantification measurements are in development. Further, this project scope includes validation and benchmarking activities of the existing capabilities of system-level thermal-hydraulic codes SAS4A/SASSYS-1 and SAM, which can be used in the development and analysis of advanced reactor technologies, ultimately supporting the licensing of these designs. This will support the licensing of new reactor designs and will allow reactor developers to reduce the conservatism they must now take in response to these uncertainties.

Prior to commencing the OKLO GAIN award testing, thermal stratification testing was performed to assess the performance of the optical fiber temperature sensors in sodium. Previous tests that were performed in deionized water were repeated. An example of the data produced during this testing can be found in Figure 41 to Figure 44.

During this particular test the flow rate was set to 5 GPM. Heater power was initially set to 0% and was tripped on at 120 seconds to 51.4% duty cycle. The heater power was maintained at 51.4% duty cycle for a period of 1000 seconds before being tripped to 0% duty cycle. Note that these tests were performed with the old SSR controller without the power meter thus the electrical power to the heater can only be estimated as 20 kWe, based on Figure 15. In Figure 41 and Figure 42 the top window of the IHX outlet window was open, whereas in Figure 43 and Figure 44 the bottom IHX outlet window was open. As can be seen, thermal stratification is evident in both the hot and cold pool in the sodium and water testing. The IHX outlet elevation has a marked effect in the thermal stratification development, with a more exaggerated stratification occurring in the water testing due to the reduced thermal conductivity of the process fluid.

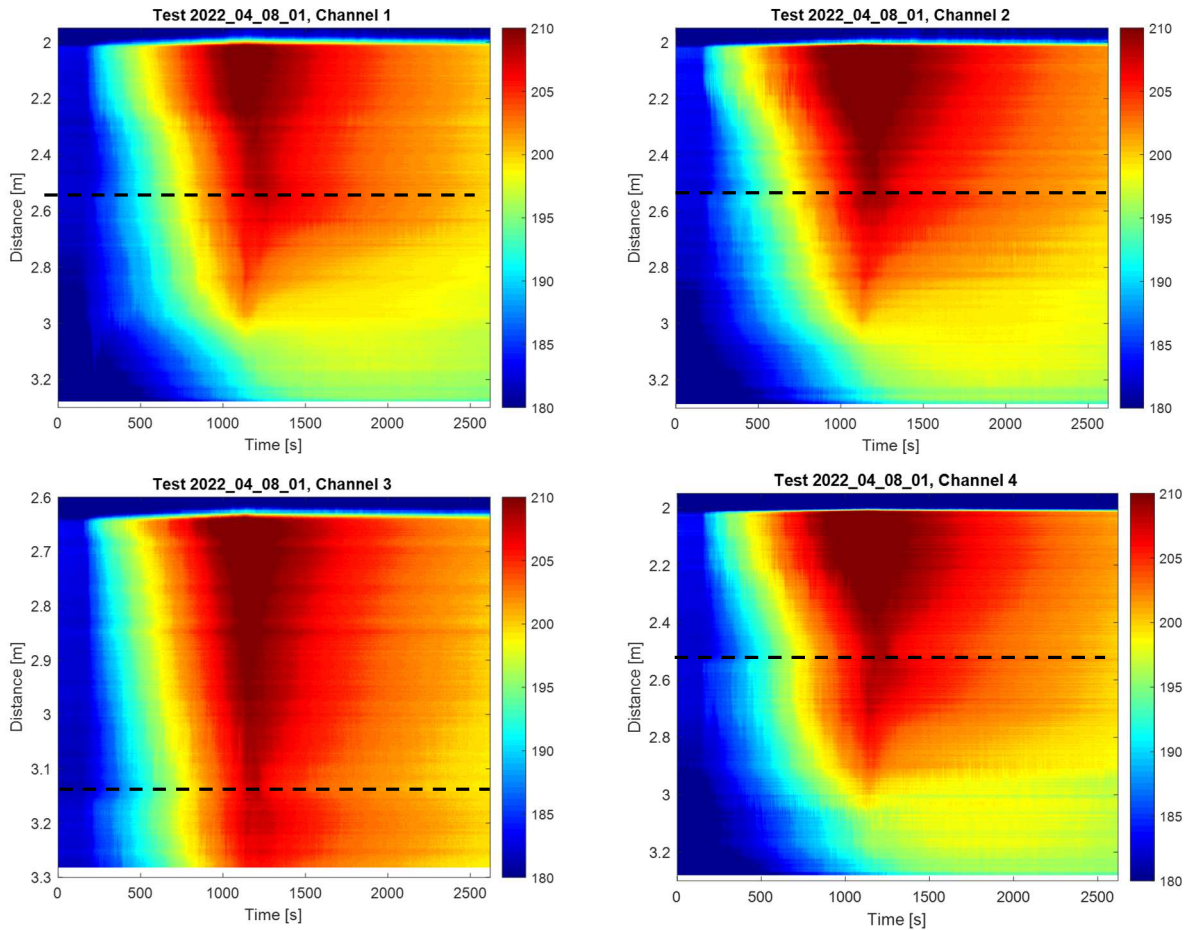


**Figure 41: Sodium testing. Temperature (°C) vs distance vs time. Sodium flowrate: 5 GPM. Heater power initially 0%, tripped on at 120 s to 51.4% duty cycle (~20 kW). Heater tripped to 0% duty cycle at 1120 s. Top IHX outlet window open**



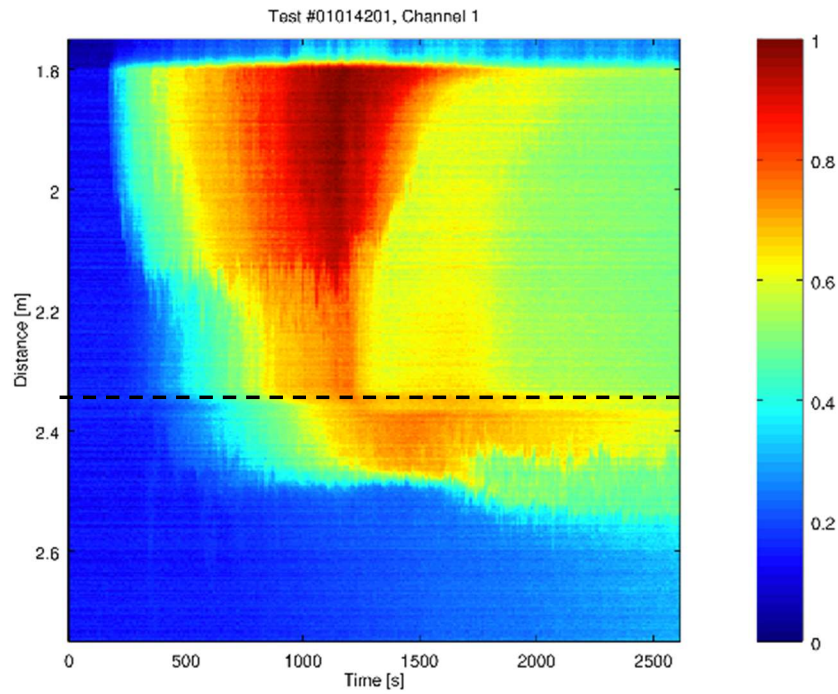


**Figure 42: Water testing. Normalized temperature (°C) vs distance vs time. water flowrate: 5 GPM. Heater power initially 0%, tripped on at 120 s to 51.4% duty cycle (~20 kWe). Heater tripped to 0% duty cycle at 1120 s. Top IHX outlet window open**

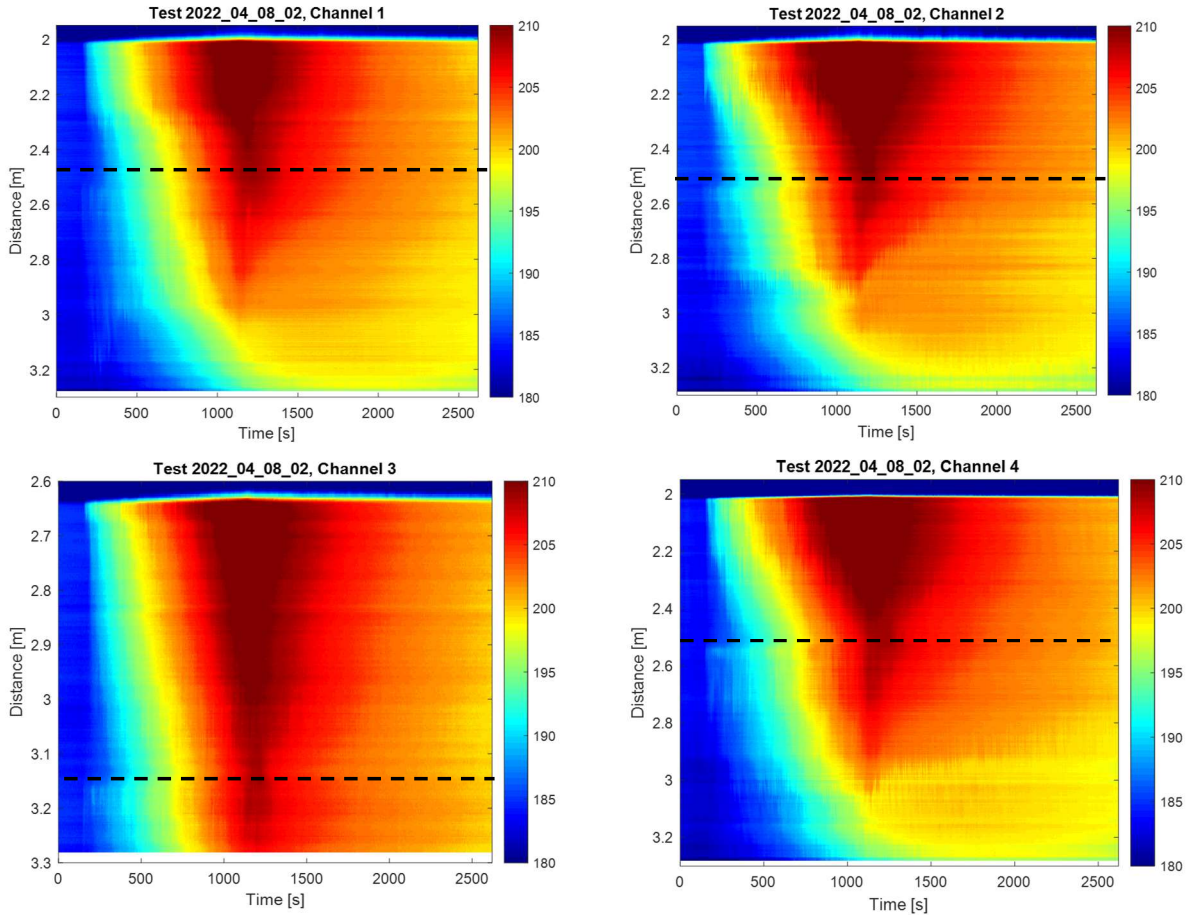


**Figure 43: Sodium testing. Temperature (°C) vs distance vs time. Sodium flowrate: 5 GPM. Heater power initially 0%, tripped on at 120 s to 51.4% duty cycle (~20 kWe). Heater tripped to 0% duty cycle at 1120 s. Bottom IHX outlet window open**

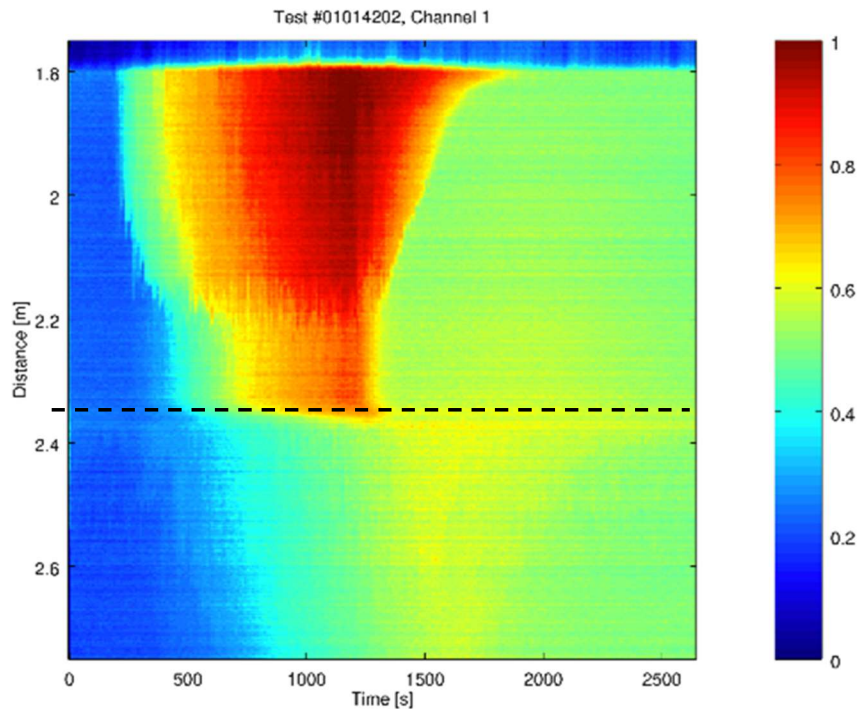


**Figure 44: Water testing. Normalized temperature (°C) vs distance vs time. Water flowrate: 5 GPM. Heater power initially 0%, tripped on at 120 s to 51.4% duty cycle (~20 kWe). Heater tripped to 0% duty cycle at 1120 s. Bottom IHX outlet window open**

## 6. THETA Model Development

Modeling of the Thermal Hydraulic Experimental Test Article (THETA) experiment has been performed using the SAS4A/SASSYS-1 fast reactor safety analysis code. A THETA model has been developed to represent the THETA experiment design developed at Argonne to demonstrate the importance of key elevations on natural circulation flow rates. The model currently includes the core channel and the primary heat transport system of the THETA experimental facility. A summary of this work can be found in [1].

## 7. Conclusions and Path Forward

All major components of the THETA primary system have been installed in METL vessel #4. All data acquisition and control systems are operational and the data acquisition and control software is functioning. The vessel was filled with sodium and an experimental campaign for THETA is being pursued. A GAIN voucher was awarded by the DOE to Oklo Inc. in partnership with Argonne (CRADA 2021-21121). THETA will continue to support the needs of industry partners. The secondary system piping and all components will be installed in FY23 to complete balance of plant.

## **8. Acknowledgements**

The authors would like to acknowledge Daniel Andujar of the METL team for all his hard work and dedication to supporting the commissioning of the THETA test article.

This work is funded by the U.S. Department of Energy Office of Nuclear Energy’s Advanced Reactor Technologies program. A special acknowledgement goes to Janelle Eddins, Advanced Reactor Development Team Lead, and Mr. Brian Robinson, Fast Reactor Program Manager for the DOE-NE ART program, for their continued support of the METL facility and its associated test articles. The authors would also like to thank Dr. Robert Hill and Dr. Bo Feng at ANL for their support. Prior years’ support has also been provided by Mr. Thomas O’Connor and Mr. Thomas Sowinski of U.S. DOE’s Office of Nuclear Energy.

## 9. References

- [1] M. Weathered *et al.*, “Thermal Hydraulic Experimental Test Article – Status Report for FY2019 Rev. 1,” Lemont, 2019.
- [2] T. Sumner and A. Moisseytsev, “Simulations of the EBR-II Tests SHRT-17 and SHRT-45R,” in *16th International Topical Meeting on Nuclear Reactor Thermal Hydraulics (NURETH-16)*, 2015.
- [3] Weathered *et al.*, “Thermal Hydraulic Experimental Test Article – Status Report FY2020,” Lemont, 2020.
- [4] M. Weathered, D. Kultgen, E. Kent, J. Rein, and C. Grandy, “Thermal Hydraulic Experimental Test Article – Fiscal Year 2021 Final Report,” Lemont, 2022.
- [5] M. Weathered, C. Grandy, M. Anderson, and D. Lisowski, “High Temperature Sodium Submersible Flowmeter Design and Analysis,” *IEEE Sens. J.*, vol. 21, no. 15, pp. 16529–16537, 2021.
- [6] Kultgen, Grandy, Hvasta, Lisowski, Toter, and Borowski, “Mechanisms Engineering Test Loop – Phase I Status Report – FY2016,” Lemont, 2016.
- [7] M. Muraoka, K. Ebata, and H. Abe, “Effect of Humidity on Small-Crack Growth in Silica Optical Fibers,” *J. Am. Ceram. Soc.*, vol. 76, 1993.
- [8] B. Prahlad and K. K. R. A. Jan, “Thermal Performance Sodium Tests Heat on a Sodium-to-Exchanger,” *J. Nucl. Sci. Technol.*, vol. 27, no. June, pp. 547–553, 1990.



## **Nuclear Science and Engineering**

Argonne National Laboratory  
9700 South Cass Avenue, Bldg. 208  
Argonne, IL 60439

[www.anl.gov](http://www.anl.gov)



Argonne National Laboratory is a U.S. Department of Energy  
laboratory managed by UChicago Argonne, LLC